International Journal of Dynamics and Control (2019) 7:256–275
https://doi.org/10.1007/s40435-018-0440-0

# Controller design scheme for stabilization and synchronization of a class of chaotic and hyperchaotic systems in uncertain environment using SMC approach

**Himesh Handa**[1] · **B. B. Sharma**[1]

Received: 28 October 2017 / Revised: 7 May 2018 / Accepted: 10 May 2018 / Published online: 25 May 2018


**Abstract**
This paper presents sliding mode control (SMC) technique for stabilization and synchronization of a class of chaotic/hyperchaotic systems in master–slave configuration. Here, a detailed procedure for deriving a single controller using SMC technique based proportional-integral sliding surface is proposed. Adaptation laws have been derived for the system parameters when the systems are subject to parametric uncertainties. Further, explicit criteria to decide the minimum number of control inputs required to meet out the desired operation of stabilization and synchronization is also proposed. Lyapunov stability theory is utilized to accomplish the desired objective. The proposed controller ensures the occurrence of sliding motion and achieves synchronization for the addressed class of chaotic/hyperchaotic systems in master–slave configuration. To validate the analytical results, example of four dimensional Lorenz–Stenflo hyperchaotic system is considered. Finally, detailed simulation results are provided to illustrate the effectiveness of the proposed controller.

**Keywords** Chaotic system · Synchronization · Sliding mode control · Lyapunov stability theory

## 1 Introduction

Controlling chaotic systems and exploiting their complex behaviour in stabilization and synchronization applications have been extensively investigated in past few decades and still this area receives a great deal of attention from research community. Since early attractors proposed by Lorenz in 1963 [1], many benchmark chaotic systems have been proposed in literature [2–5]. Control of these chaotic systems and their applications are widely explored since the pioneer work of Ott, Grebogi and York (OGY) on chaos control [6]. Chaotic systems are dynamical systems that are highly sensitive to initial conditions and parametric variations. As a result, these systems display complex noise like unpredictable behaviour. Due to the presence of more than one positive Lyapunov exponents, generally, hyperchaotic systems exhibit more complex dynamical behaviour than chaotic systems. Different hyperchaotic systems and associated complex behaviours are reported in literature [7–14]. In context to chaotic/hyperchaotic systems, their complex unpredictable behaviour may be undesirable and may adversely affect the operation and performance of electrical and mechanical systems [15]. This complex dynamical behaviour may sometimes induce unwanted oscillations resulting in resonance which can lead to physical damage in some systems. Suppression of chaotic behaviour in mechanical systems has been intensively studied by many researchers. Suppression of chaos in micro-electromechanical system resonators have been presented by Shang et al. in [16]. Several studies have investigated the nonlinear dynamics in magnetically levitated systems [17,18]. Therefore, chaos stabilization is of special importance and can be observed in systems involving chemical reactions [19,20], biological systems [21–25], applied physics [26–28] etc. Keeping in view all these contributions, it can be concluded that chaos control and suppression have been addressed a great deal over the last few decades. Further studies related to suppression of chaotic oscillations can be found in [29–31] and the references therein.

Along with chaos control, synchronization of chaotic/hyperchaotic systems has also attracted tremendous interest of

✉ Himesh Handa
hklhanda@gmail.com

B. B. Sharma
bharat.nit@gmail.com

[1] Electrical Engineering Department, National Institute of Technology, Hamirpur, HP 177005, India

many researchers keeping in view its possible applications in secure communication [32,40,41,44]. Concept of synchronization of chaotic systems was first studied and presented by Pecora and Carroll [33,34]. Chaotic system synchronization deals with the possibility of two or more chaotic systems oscillating in a synchronized manner [35,36]. In literature, various types of synchronization phenomenon have been studied such as complete synchronization, phase synchronization, partial synchronization, generalized synchronization and projective synchronization etc. [37–40]. These schemes find applications in many potential fields like secure communication, neural networks, optimization of nonlinear system performance, modelling brain activity, system identification and pattern recognition etc. [41–43]. In secure communication, due to the presence of highly complex attractor, hyperchaotic systems are preferred to enhance the security in communication applications by generating more complex dynamics [44]. In order to synchronize chaotic systems, many effective control techniques like active control [45], contraction theory [46,47], backstepping design method [48], adaptive control [49], feedback linearization [50], sliding mode control [51–56] etc. have been used.

To deal with stabilization and synchronization of uncertain chaotic/hyperchaotic systems, sliding mode control approach has been widely used in literature [51–56]. Active sliding mode control based technique to realize synchronization of chaotic systems with parametric uncertainty is proposed by Zhang et al. [52]. The sufficient condition to ensure robust stability of error dynamics is explored in this work. A robust sliding mode control scheme for the synchronization of unified chaotic systems is presented by Yan et al. in [53]. In there work, a novel proportional integral (PI) switching surface is introduced for determining the synchronization performance of the system in sliding motion. Chaos control for uncertain unified chaotic system by means of sliding mode control approach is addressed by Ablay in [54]. Roopaei et al. in [55] introduced a class of unknown chaotic systems and have utilized an adaptive sliding mode controller to stabilize the new chaotic class. Design of adaptive sliding mode control scheme for the synchronization of Genesio–Tesi chaotic system is proposed by Ghamati et al. in [56]. Further a switching surface is proposed and based on the selection of switching surface, two sliding mode control schemes have been presented to ensure the occurrence of sliding motion.

To the best of our knowledge, majority of the works available on SMC based stabilization and synchronization targets only third order chaotic systems and utilize more than one control inputs and are confined to some specific chaotic systems like unified system, Genesio–Tesi system etc. However, in the present work, sliding mode control scheme is utilized to address the problem of stabilization and complete synchronization for a wider class of chaotic as well as hyperchaotic systems. Based on Lyapunov stability analysis, a framework for deriving single controller structure to address the synchronization problem with and without uncertainties in system parameters is developed. To ensure the occurrence of sliding motion, a proportional-integral (PI) switching surface is also derived. Moreover, attempt has also been made to develop explicit criteria to decide the minimum number of control inputs required to meet out the objective of stabilization and synchronization. Numerical example showing the detailed design methodology is presented for hyperchaotic Lorenz–Stenflo system. Simulations are presented at the end to show the convergence behaviour of system states as well as the time evolution of uncertain system parameters. The proposed methodology can be easily adopted to address other systems as well which are not part of identified class with slight modification of procedure. In this regard, necessary remarks are made in the paper at appropriate places. Overall, key contributions of this paper can be summarized as follows:

i. Detailed analytical procedure for deriving single stabilizing controller using SMC technique based on PI sliding surface for identified class of chaotic and hyperchaotic systems is proposed and
ii. The procedure is extended to achieve two system synchronization using single controller.
iii. Analytical results for controller design and adaptation laws for parameters are derived when the systems are subjected to limited parametric uncertainty and global asymptotic stability is established in all cases using Lyapunov stability theory. Finally, Simulation results to support the analytical results are presented to highlight the efficacy of proposed strategy.

This paper is organized as follows: In Sect. 2, problem formulation for stabilizing a class of chaotic/hyperchaotic systems is presented. Detailed procedure for addressing the synchronization problem for the same class of systems is presented in Sect. 3. Section 4, presents analytical results for adaptive synchronization when systems are subjected to parametric uncertainties. Section 5, deals with the description of fourth order hyperchaotic Lorenz–Stenflo system taken as an example to validate the derived results. Further, in this section, the results derived in previous section are applied to achieve stabilization and synchronization of chaotic systems in master–slave configuration. Detailed numerical simulations showing the effectiveness of the applied approach are presented in Sect. 6. Finally, Sect. 7 concludes the contribution made in this paper.

## 2 Problem formulation for stabilization problem

In this section, problem formulation for the stabilization of proposed class of chaotic/hyperchaotic systems using sliding mode control technique is given. Lyapunov stability analysis is used to derive the analytical results related to the design of proportional-integral (PI) switching surface and associated control law.

### 2.1 SMC based stabilizing controller design

In the present subsection, the basic application of SMC approach to stabilization problem is highlighted, which is commonly adopted in majority of control literature. To develop sliding mode control (SMC) based stabilization controller design procedure, consider the following class of nonlinear systems:

$$\dot{\boldsymbol{x}} = A\boldsymbol{x} + B\boldsymbol{f}(\boldsymbol{x}) \tag{1}$$

where $\boldsymbol{x} \in \Re^n$ is the state vector, $A \in \Re^{n\times n}$ is matrix of system parameters , $B \in \Re^{n\times n}$ is matrix associated with nonlinear part of system dynamics and $\boldsymbol{f} : \Re^n \to \Re^n$ is a nonlinear vector function of system states.

In stabilization of a system, the idea is to design an appropriate control input $\boldsymbol{u} \in \Re^m$, such that under the effect of the designed control function, the states of the system converge to equilibrium point or origin.

To achieve this goal, the dynamics of system (1) with stabilizing controller $\boldsymbol{u}$ can be written as

$$\dot{\boldsymbol{x}} = A\boldsymbol{x} + B\boldsymbol{f}(\boldsymbol{x}) + D\boldsymbol{u} \tag{2}$$

where $D \in \Re^{n\times m}$ is a matrix having non-zero entries corresponding to the dynamics of those states to which the control term is required to be associated to meet out the stabilization requirements.

Here, the objective is to design the control input $u \in \Re^m$ such that system states are stabilized i.e.

$$\lim_{t\to\infty} \|\boldsymbol{x}(t)\| \to 0 \tag{3}$$

By suitably selecting the proportional-integral (PI) based sliding surfaces $s_i(t) = 0$, for $i = 1, 2, \ldots, m$, and $m < n$, the original system dynamics in (1) can be replaced by an equivalent dynamics expressed as follows:

$$\dot{\boldsymbol{x}}(t) = A'\boldsymbol{x}(t) + B'\boldsymbol{f}'(\boldsymbol{x}(t)) \tag{4}$$

The selection of sliding surfaces is made such that the Lyapunov function $V_1(\boldsymbol{x}(t)) = \boldsymbol{x}^T\boldsymbol{x}$ establishes the following stability condition for the modified system dynamics in (4):

$$\dot{V}_1(\boldsymbol{x}(t)) \leq 0 \tag{5}$$

Further, in order to drive the system trajectories to the sliding surfaces $s_i(t) = 0$, for $i = 1, 2, \ldots .m$, proper selection of the control inputs $u_i(t)$ is required to be made. This is achieved by selecting new Lyapunov function defined as

$$V_2(s_i(t)) = 0.5s_i^2(t); \quad i = 1, 2, \ldots, m \tag{6}$$

and then establishing

$$\dot{V}_2(s_i(t)) < 0; \quad i = 1, 2, \ldots, m \tag{7}$$

It guarantees the existence of sliding mode for the system given in (1). Based on the above preliminary description, the main results of the paper are derived in the subsequent sections.

### 2.2 Procedure to design stabilization controller for a class of chaotic/hyperchaotic systems

In this subsection, procedure for the selection of controllers and appropriate switching surfaces is elaborated for a class of chaotic/hyperchaotic systems. In order to design suitable SMC based controller and appropriate sliding surface, the sub-class of nonlinear systems belonging to the wider class presented in (1) is considered as follows:

$$\dot{x}_i = \sum_{k=1}^{n} \theta_{ik}x_k + \sum_{j=2}^{n} F_{ij}; \quad i = 1, 2, 3, \ldots, n \tag{8}$$

here $x_i$ is the $i$th state variable of the system, elements $\theta_{ik}$ are linked to the actual system parameters and are coefficients associated with linear part of dynamics with $\theta_{ii} < 0$ for $i = 1, 2, 3, \ldots, n$, which will constitute the entries of $A$ matrix in (1) and $\sum_{j=2}^{n} F_{ij}$ is the nonlinear part of the system associated with $i$th state space equation. The above description covers a variety of chaotic/hyperchaotic systems like chaotic Lorenz system [57], four dimensional hyperchaotic Lorenz type system [58], Lorenz–Stenflo system [59,60] etc. These systems have product type quadratic terms as part of nonlinearities. The dynamics of the nonlinear system (8) with controller applied to the $l$th state equation of the system can be represented as follows:

$$\begin{cases} \dot{x}_1 = \sum_{k=1}^{n} \theta_{1k} x_k + \sum_{j=2}^{n} F_{1j} \\ \dot{x}_2 = \sum_{k=1}^{n} \theta_{2k} x_k + \sum_{j=2}^{n} F_{2j} \\ \vdots \\ \dot{x}_l = \sum_{k=1}^{n} \theta_{lk} x_k + \sum_{j=2}^{n} F_{lj} + u_l \\ \dot{x}_{l+1} = \sum_{k=1}^{n} \theta_{l+1,k} x_k + \sum_{j=2}^{n} F_{l+1,j} \\ \vdots \\ \dot{x}_n = \sum_{k=1}^{n} \theta_{nk} x_k + \sum_{j=2}^{n} F_{nj} \end{cases} \tag{9}$$

The description in Eq. (9) has product type nonlinearities defined as $F_{ij} = x_1 \left( -\sum_{j=2, j>i}^{n} x_j + \sum_{j=2, j<i}^{n} x_j \right)$; for $i = 1, 2, 3, \ldots, n$.

**Assumption 1** For the class of nonlinear system described in (8), following assumptions are taken:

- All diagonal entries of the system matrix $A$ associated with linear part are negative i.e. in matrix $A = \begin{bmatrix} \theta_{11} & \theta_{12} & \cdots & \theta_{1n} \\ \theta_{21} & \theta_{22} & \cdots & \theta_{2n} \\ \vdots & \vdots & \cdots & \vdots \\ \theta_{n1} & \theta_{n2} & \cdots & \theta_{nn} \end{bmatrix}$; $\theta_{ii} < 0, \quad \forall i = 1, 2, 3, \ldots, n.$
- The rest of the entries of matrix $A$ are such that for $i = l$, $\theta_{lj} \neq 0$, for some $j$ and $\theta_{lj} \neq -\theta_{jl}$ for all non-zero $\theta_{lj}$. Further, $\theta_{ij} = \theta_{ji} = 0$ or $\theta_{ij} = -\theta_{ji}$; $\forall i \neq l$.

***Remark 1*** The Assumption 1 is followed by the members of proposed class of systems in (9) and it helps in deriving detailed procedure for stabilizing controller design analytically.

***Remark 2*** The proposed strategy can be extended to other systems which deviate in description as given in (8). If $\theta_{ii} > 0$ for any $i$, then single controller is needed if assumption 1 is also true for $l = i$.

***Remark 3*** For the case, where $l \neq i$, two controllers $u_i$ and $u_l$ are required to be used along with two sliding surfaces $s_i$ and $s_l$ and the procedure as per Sect. 2.1 can be easily adopted for such cases.

To achieve this objective using SMC approach, selection of appropriate switching surface is made which guarantees the stability of the equivalent dynamics as in (4) in sliding mode so that the system states converge to zero. Then, a sliding mode control law is established, which guarantees the existence of sliding surface $s_l = 0$.

In order to ensure asymptotic stability of sliding mode, the proportional-integral switching surface $s_l$ can be selected as follows:

$$s_l = x_l + \int_0^t \left\{ \beta_1 x_l + \sum_{i=1, i\neq l}^{n} \theta_{il} x_i + \frac{1}{x_l} \left( \sum_{i=1, i\neq l}^{n} x_i \sum_{j=2}^{n} F_{ij} \right) \right\} d\tau \tag{10}$$

where $\beta_1$ is a positive constant to be specified by the designer, appropriately. When the system operates in sliding mode, following Utkin condition [61] holds:

$$\dot{s}_l = 0 \tag{11}$$

From (10), sliding mode dynamics can be obtained as follows:

$$\dot{s}_l = \dot{x}_l + \beta_1 x_l + \sum_{i=1,\ i\neq l}^{n} \theta_{il} x_i + \frac{1}{x_l} \left( \sum_{i=1,\ i\neq l}^{n} x_i \sum_{j=2}^{n} F_{ij} \right) \tag{12}$$

Using (12), one can write

$$\dot{x}_l = -\beta_1 x_l - \sum_{i=1, i\neq l}^{n} \theta_{il} x_i - \frac{1}{x_l} \left( \sum_{i=1, i\neq l}^{n} x_i \sum_{j=2}^{n} F_{ij} \right) \tag{13}$$

Therefore, the equivalent sliding mode dynamics can be written as follows:

$$\begin{cases} \dot{x}_1 = \sum_{k=1}^{n} \theta_{1k} x_k + \sum_{j=2}^{n} F_{1j} \\ \dot{x}_2 = \sum_{k=1}^{n} \theta_{2k} x_k + \sum_{j=2}^{n} F_{2j} \\ \vdots \\ \dot{x}_l = -\beta_1 x_l - \sum_{i=1,\ i\neq l}^{n} \theta_{il} x_i - \frac{1}{x_l} \left( \sum_{i=1,\ i\neq l}^{n} x_i \sum_{j=2}^{n} F_{ij} \right) \\ \dot{x}_{l+1} = \sum_{k=1}^{n} \theta_{l+1,k} x_k + \sum_{j=2}^{n} F_{l+1,j} \\ \vdots \\ \dot{x}_n = \sum_{k=1}^{n} \theta_{nk} x_k + \sum_{j=2}^{n} F_{nj} \end{cases} \tag{14}$$

To ensure the occurrence of sliding motion and stabilization of the system dynamics, PI based sliding mode controller $u_l$ in (9) is required to be suitably designed.

**Theorem 1** *For the system state description in (9), for any $i = l$, the PI sliding surface selected as in (10) along with a single sliding mode controller selected as*

$$u_l = -\sum_{k=1}^{n} \theta_{lk} x_k - \sum_{j=2}^{n} F_{lj} - \beta_1 x_l$$

$$- \sum_{i=1,i\neq l}^{n} \theta_{il} x_i - \frac{1}{x_l} \left( \sum_{i=1,i\neq l}^{n} x_i \sum_{j=2}^{n} F_{ij} \right) - \sigma sign\,(s_l)\,;\, \sigma > 0 \tag{15}$$

*Associated with l*th *state of the system dynamics are sufficient to ensure convergence of system trajectories to the sliding surface* $s_l = 0$. *Further, global asymptotic stabilization (GAS) of the state trajectories is achieved with control function (15) i.e.* $\lim_{t\to\infty} \|x_i\,(t)\| \to 0$, *for* $i = 1, 2, 3, \ldots, n$.

***Proof*** For the modified dynamics in (14), the stability of sliding mode dynamics is analyzed using Lyapunov stability theory. For this purpose, let the Lyapunov function candidate be selected as follows:

$$V_3 = 0.5 \left( \sum_{i=1}^{n} x_i^2 \right) \tag{16}$$

The time derivative of Lyapunov function in (16), along the trajectories of system in (14), can be written as follows:

$$\begin{aligned}
\dot{V}_3 &= \sum_{i=1}^{n} x_i \dot{x}_i = x_l \dot{x}_l + \sum_{i=1,\ i\neq l}^{n} x_i \dot{x}_i \\
&= x_l \dot{x}_l + \sum_{i=1,\ i\neq l}^{n} x_i \left( \sum_{k=1}^{n} \theta_{ik} x_k + \sum_{j=2}^{n} F_{ij} \right) \\
&= x_l \dot{x}_l + \sum_{i=1,\ i\neq l}^{n} x_i \sum_{k=1}^{n} \theta_{ik} x_k \\
&\quad + \sum_{i=1,\ i\neq l}^{n} x_i \sum_{j=2}^{n} F_{ij} \\
&= x_l \dot{x}_l + x_l \sum_{i=1,\ i\neq l}^{n} \theta_{il} x_i \\
&\quad + \sum_{i=1,\ i\neq l}^{n} x_i \sum_{k=1,\ k\neq l}^{n} \theta_{ik} x_k \\
&\quad + \sum_{i=1,\ i\neq l}^{n} x_i \sum_{j=2}^{n} F_{ij} \\
\Rightarrow \dot{V}_3 &= x_l \left( \dot{x}_l + \sum_{i=1,\ i\neq l}^{n} \theta_{il} x_i \right. \\
&\quad \left. + \frac{1}{x_l} \left\{ \sum_{i=1,\ i\neq l}^{n} x_i \sum_{j=2}^{n} F_{ij} \right\} \right) \\
&\quad + \sum_{i=1,\ i\neq l}^{n} x_i \sum_{k=1,\ k\neq l}^{n} \theta_{ik} x_k
\end{aligned}$$

Using $\dot{x}_l$ from (13), $\dot{V}_3$ reduces to

$$\dot{V}_3 = -\beta_1 x_l^2 + \sum_{i=1,\ i\neq l}^{n} x_i \sum_{k=1,\ k\neq l}^{n} \theta_{ik} x_k = -\boldsymbol{\xi}^T P \boldsymbol{\xi} \leq 0 \tag{17}$$

where $\boldsymbol{\xi} = \begin{bmatrix} x_1 & x_2 & \cdots & x_n \end{bmatrix}^T$ is state vector. The matrix $P$ turns out to be a real symmetric matrix in (17) which can be expressed as follows:

$$P = \begin{bmatrix}
-\theta_{11} & \frac{(\theta_{12}+\theta_{21})}{2} & \cdots & 0 & \cdots & \frac{(\theta_{1n}+\theta_{n1})}{2} \\
\frac{(\theta_{21}+\theta_{12})}{2} & -\theta_{22} & \cdots & 0 & \cdots & \frac{(\theta_{2n}+\theta_{n2})}{2} \\
\vdots & \vdots & \vdots & \vdots & \vdots & \vdots \\
0 & 0 & \cdots & \beta_1 & \cdots & 0 \\
\vdots & \vdots & \vdots & \vdots & \vdots & \vdots \\
\frac{(\theta_{n1}+\theta_{1n})}{2} & \frac{(\theta_{n2}+\theta_{2n})}{2} & \cdots & 0 & \cdots & -\theta_{nn}
\end{bmatrix} \tag{18}$$

As per Assumption 1, all the diagonal entries of the system matrix $A$ in (1) are negative and by selecting design gain $\beta_1 > 0$, the real symmetric matrix $P$ reduces to following:

$$P = \begin{bmatrix}
-\theta_{11} & 0 & \cdots & 0 & \cdots & 0 \\
0 & -\theta_{22} & \cdots & 0 & \cdots & 0 \\
\vdots & \vdots & \vdots & \vdots & \vdots & \vdots \\
0 & 0 & \cdots & \beta_1 & \cdots & 0 \\
\vdots & \vdots & \cdots & \vdots & \vdots & \vdots \\
0 & 0 & 0 & 0 & 0 & -\theta_{nn}
\end{bmatrix}$$

which is positive definite matrix.

With $\theta_{ii} < 0$ and $P$ being positive definite matrix in (17), it can be established that the zero equilibrium point $(x_1 = x_2 \ldots = x_n = 0)$ of the system (9) is globally asymptotically stable (GAS) as the Lyapunov function is radially bounded [62–64].

To ensure that the system states are directed towards the sliding surface (10), if the controller $u_l$ in (15) is applied to the $l$th state of the system (9), then the system states converge to the sliding surface ensuring that $\lim_{t\to\infty} \|x_i\| \to 0$, for $i = 1, 2, 3, \ldots, n$.

In order to accomplish the objective of convergence of system trajectories to sliding surface, consider new Lyapunov function as

$$V_4 = 0.5 s_l^2 \tag{19}$$

Taking time derivative of (19) and using (9) and (12), one can get

$$\dot{V}_4 = s_l \dot{s}_l$$

$$= s_l \left( \dot{x}_l + \beta_1 x_l + \sum_{i=1,\ i\neq l}^{n} \theta_{il} x_i + \frac{1}{x_l} \left( \sum_{i=1,\ i\neq l}^{n} x_i \sum_{j=2}^{n} F_{ij} \right) \right)$$

$$= s_l \left( \sum_{k=1}^{n} \theta_{lk} x_k + \sum_{j=2}^{n} F_{lj} + \beta_1 x_l + \sum_{i=1,\ i\neq l}^{n} \theta_{il} x_i + \frac{1}{x_l} \left( \sum_{i=1,\ i\neq l}^{n} x_i \sum_{j=2}^{n} F_{ij} \right) + u_l \right)$$

Using the control function $u_l$ as given in (15), one can get

$$\dot{V}_4 \leq -s_l \sigma sign\,(s_l) \leq -\sigma\,|s_l| \tag{20}$$

As $\dot{V}_4 \leq 0$, thus, according to Lyapunov stability analysis, all the system trajectories converge to the sliding surface and the state dynamics in the sliding mode is asymptotically stable, which implies that $\lim_{t\to\infty} \|x_i\,(t)\| \to 0$, for $i = 1, 2, 3, \ldots, n$.

Thus, objective of stabilization of class of system in (9) is accomplished. □

## 3 Problem formulation for SMC based synchronizing controller design

In this section, basic formulation for synchronizing controller design for two chaotic/hyperchaotic systems in master–slave configuration is presented and later on, detailed procedure for a sub-class of chaotic/hyperchaotic systems as in (9) in master–slave configuration is proposed.

For the synchronization of nonlinear dynamical systems (chaotic systems/hyperchaotic systems) in master–slave configuration, consider the dynamics of the master system as follows:

$$\dot{\boldsymbol{x}} = A\boldsymbol{x} + B\boldsymbol{f}\,(\boldsymbol{x}) \tag{21}$$

where $\boldsymbol{x} \in \Re^n$ is the state vector of the master system, $A \in \Re^{n\times n}$ is matrix of system parameters, $B \in \Re^{n\times n}$ is matrix associated with nonlinear part of system dynamics and $\boldsymbol{f} : \Re^n \to \Re^n$ is a nonlinear vector function of states of the master system.

By associating the control input signal $\boldsymbol{u} \in \Re^m$ suitably, the controlled dynamics of the slave system can be expressed as follows:

$$\dot{\boldsymbol{y}} = A\boldsymbol{y} + B\boldsymbol{f}\,(\boldsymbol{y}) + D\boldsymbol{u} \tag{22}$$

where $\boldsymbol{y} \in \Re^n$ is the state vector of the slave system, $A \in \Re^{n\times n}$ is matrix of system parameters , $B \in \Re^{n\times n}$ is matrix associated with nonlinear part of slave system dynamics and $\boldsymbol{f} : \Re^n \to \Re^n$ is a nonlinear vector function of slave system states. Here, again $D \in \Re^{n\times m}$ is a matrix with non-zero entries corresponding to the states to which the control function is required to be associated to meet out the objective of synchronization in master–slave configuration.

In synchronization problem, idea is to identify the control input or signal $\boldsymbol{u} \in \Re^m$ such that the trajectories of the slave system follow the trajectories of the master system or the control input is designed in such a way that makes the slave system states to evolve in a similar manner as that of the master system with time. Synchronization in master–slave configuration can be shown by Fig. 1, where error between the states of the identical master and slave system is used as driving signal. Thus when $\boldsymbol{y} \to \boldsymbol{x}$, then $\boldsymbol{e} \to 0$, which implies that the objective of synchronization has been achieved.

To achieve this objective, error between the states of master system and slave system is defined as follows:

$\boldsymbol{e} = \boldsymbol{y} - \boldsymbol{x}$, where $\boldsymbol{e}^T = \begin{bmatrix} e_1 & e_2 & \ldots & e_n \end{bmatrix}$.

Using above definition, the synchronization error dynamics using Eqs. (21) and (22) is obtained as:

$$\begin{aligned} \dot{\boldsymbol{e}} = \dot{\boldsymbol{y}} - \dot{\boldsymbol{x}} &= A\boldsymbol{y} + B\boldsymbol{f}\,(\boldsymbol{y}) + D\boldsymbol{u} - A\boldsymbol{x} - B\boldsymbol{f}\,(\boldsymbol{x}) \\ &= A\,(\boldsymbol{y}\text{-}\boldsymbol{x}) + B\,(\boldsymbol{f}\,(\boldsymbol{y}\,) - \boldsymbol{f}\,(\,\boldsymbol{x})) + D\boldsymbol{u} \\ &= A\boldsymbol{e} + B\boldsymbol{h}\,(\boldsymbol{x},\boldsymbol{y}) + D\boldsymbol{u} \end{aligned} \tag{23}$$

where vector function $\boldsymbol{h}\,(\boldsymbol{x},\boldsymbol{y}) = (\boldsymbol{f}\,(\boldsymbol{y}) - \boldsymbol{f}\,(\boldsymbol{x}))$, accommodates the nonlinear terms of both master and slave systems.

Here the objective is to design the controller $\boldsymbol{u} \in \Re^m$ such that

$$\lim_{t\to\infty} \|\boldsymbol{e}\,(t)\| \to 0 \tag{24}$$

First of all, suitable selection of the sliding surfaces $s_i\,(t) = 0$ is made for $i = 1, 2, \ldots, m$ i.e.

$$s_i\,(t) = f_i\,(\boldsymbol{e}\,(t)\,, \boldsymbol{y}) = 0 \tag{25}$$

To maintain the system trajectories in sliding mode, it is ensured that $\dot{s}_i\,(t) = 0$. Further, the modified or equivalent dynamics of the error system can be written as:

$$\dot{\boldsymbol{e}}\,(t) = A'\boldsymbol{e}\,(t) + \boldsymbol{h}'\,(\boldsymbol{e}\,(t)\,, \boldsymbol{y}) \tag{26}$$

The selection of sliding surface $s_i\,(t)$ is made such that Lyapunov function $V_5\,(\boldsymbol{e}\,(t)) = \boldsymbol{e}^T\boldsymbol{e}$ establishes following asymptotic stability condition:

$$\dot{V}_5\,(\boldsymbol{e}\,(t)) \leq 0 \tag{27}$$

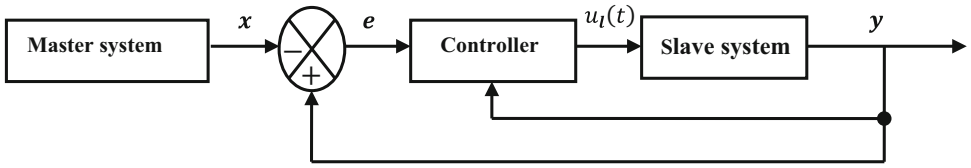


**Fig. 1** Complete synchronization scheme in master–slave configuration

In addition to the selection of the appropriate sliding surface, selection of the control input $u_i\,(t)$ has to be done so that system trajectories are driven and confined to the sliding surfaces $s_i\,(t) = 0$, for $i = 1, 2, \ldots, m$.

To achieve this goal, selection of the new Lyapunov function is made as follows:

$$V_6\,(s_i\,(t)) = 0.5 s_i^2\,(t)\,; \quad i = 1, 2, \ldots, m \tag{28}$$

Further, by selecting $u_i\,(t)$ appropriately, time derivative of $V_6\,(s_i\,(t))$ may be shown to be negative definite i.e.

$$\dot{V}_6\,(s_i\,(t)) < 0 \tag{29}$$

The above result ensures the existence of sliding mode for the synchronization problem under consideration and implies that the error dynamics in sliding manifold is asymptotically stable according to (27), which shows that $\lim_{t\to\infty} \|\boldsymbol{e}\,(t)\| \to 0$ and the master and the slave systems are synchronized with each other.

### 3.1 Procedure for the synchronization of proposed class of systems

In order to achieve the objective of synchronization using sliding mode control approach, the dynamics of the sub-class described in (8) is considered as master system.

Similarly, the dynamics of the slave system can be written as

$$\dot{y}_i = \sum_{k=1}^{n} \theta_{ik} y_k + \sum_{j=2}^{n} F'_{ij}; \quad i = 1, 2, 3, \ldots, n. \tag{30}$$

here $y_i$ represent the $i$th state variable and $\theta_{ik}$'s are the coefficients associated with the linear part of the system dynamics with $\theta_{ii} < 0$, which will constitute the entries of system matrix $A$ of (22) similar to master system case. $\sum_{j=2}^{n} F'_{ij} = y_1 \left( -\sum_{j=2, j>i}^{n} y_j + \sum_{j=2, j<i}^{n} y_j \right)$ is the nonlinear part of the system.

The master system dynamics is similar to the system considered in (9) and is reproduced here:

$$\begin{cases} \dot{x}_1 = \sum_{k=1}^{n} \theta_{1k} x_k + \sum_{j=2}^{n} F_{1j} \\ \dot{x}_2 = \sum_{k=1}^{n} \theta_{2k} x_k + \sum_{j=2}^{n} F_{2j} \\ \vdots \\ \dot{x}_l = \sum_{k=1}^{n} \theta_{lk} x_k + \sum_{j=2}^{n} F_{lj} \\ \dot{x}_{l+1} = \sum_{k=1}^{n} \theta_{l+1,k} x_k + \sum_{j=2}^{n} F_{l+1,j} \\ \vdots \\ \dot{x}_n = \sum_{k=1}^{n} \theta_{nk} x_k + \sum_{j=2}^{n} F_{nj} \end{cases} \tag{31}$$

Similarly, the dynamics of the slave system with controller applied to the $l$th state of the slave system dynamics can be expressed as follows:

$$\begin{cases} \dot{y}_1 = \sum_{k=1}^{n} \theta_{1k} y_k + \sum_{j=2}^{n} F'_{1j} \\ \dot{y}_2 = \sum_{k=1}^{n} \theta_{2k} y_k + \sum_{j=2}^{n} F'_{2j} \\ \vdots \\ \dot{y}_l = \sum_{k=1}^{n} \theta_{lk} y_k + \sum_{j=2}^{n} F'_{lj} + u_l \\ \dot{y}_{l+1} = \sum_{k=1}^{n} \theta_{l+1,k} y_k + \sum_{j=2}^{n} F'_{l+1}, j \\ \vdots \\ \dot{y}_n = \sum_{k=1}^{n} \theta_{nk} y_k + \sum_{j=2}^{n} F'_{nj} \end{cases} \tag{32}$$

To establish complete synchronization between master system (31) and the slave system (32), the error can be defined as follows:

$$e_i = y_i - x_i; \quad i = 1, 2, 3, \ldots, n. \tag{33}$$

Using the dynamics in (31) and (32), the resulting error dynamics can be written as follows:

$$\begin{cases} \dot{e}_1 = \sum_{k=1}^{n} \theta_{1k} e_k + \sum_{j=2}^{n} \Psi_{1j} \\ \dot{e}_2 = \sum_{k=1}^{n} \theta_{2k} e_k + \sum_{j=2}^{n} \Psi_{2j} \\ \vdots \\ \dot{e}_l = \sum_{k=1}^{n} \theta_{lk} e_k + \sum_{j=2}^{n} \Psi_{lj} + u_l \\ \dot{e}_{l+1} = \sum_{k=1}^{n} \theta_{l+1,k} e_k + \sum_{j=2}^{n} \Psi_{l+1,j} \\ \vdots \\ \dot{e}_n = \sum_{k=1}^{n} \theta_{nk} e_k + \sum_{j=2}^{n} \Psi_{nj} \end{cases} \tag{34}$$

Here, nonlinear function $\Psi_{ij} = y_1 \left( - \sum_{j=2, j>i}^{n} e_j + \sum_{j=2, j<i}^{n} e_j \right) + e_1 \left( - \sum_{j=2, j>i}^{n} y_j + \sum_{j=2, j<i}^{n} y_j \right) + e_1 \left( \sum_{j=2, j>i}^{n} e_j - \sum_{j=2, j<i}^{n} e_j \right)$; for $i = 1, 2, 3, \ldots, n$.

The uncontrolled trajectories of the nonlinear systems described in (31) and (32) will separate out quickly, with different initial conditions, being member of assumed chaotic/hyperchaotic class. Therefore, in order to synchronize two systems in master–slave configuration one has to design a suitable SMC based controller such that $\lim_{t\to\infty} \| \boldsymbol{e}(t) \| \to 0 \Rightarrow \lim_{t\to\infty} \| e_1 \; e_2 \cdots e_n \| \to 0$.

To ensure that the slave system follows the trajectories of the master system, leading to meet out the objective of synchronization, the proportional-integral switching surface $s_l$ can be selected as follows:

$$s_l = e_l + \int_0^t \left\{ \beta_1 e_l + \sum_{i=1, i\neq l}^{n} \theta_{il} e_i + \frac{1}{e_l} \left( \sum_{i=1, i\neq l}^{n} e_i \sum_{j=2}^{n} \Psi_{ij} \right) \right\} d\tau \tag{35}$$

where $\beta_1$ is a positive constant to be suitably selected by the designer. When the system operates in sliding mode $\dot{s}_l = 0$, the following equation holds:

$$\dot{s}_l = \dot{e}_l + \beta_1 e_l + \sum_{i=1, i\neq l}^{n} \theta_{il} e_i + \frac{1}{e_l} \left( \sum_{i=1, i\neq l}^{n} e_i \sum_{j=2}^{n} \Psi_{ij} \right) = 0 \tag{36}$$

It further implies that

$$\dot{e}_l = -\beta_1 e_l - \sum_{i=1, i\neq l}^{n} \theta_{il} e_i - \frac{1}{e_l} \left( \sum_{i=1, i\neq l}^{n} e_i \sum_{j=2}^{n} \Psi_{ij} \right) \tag{37}$$

Therefore, from (34) and (37), the equivalent sliding mode dynamics can be written as follows:

$$\begin{cases} \dot{e}_1 = \sum_{k=1}^{n} \theta_{1k} e_k + \sum_{j=2}^{n} \Psi_{1j} \\ \dot{e}_2 = \sum_{k=1}^{n} \theta_{2k} e_k + \sum_{j=2}^{n} \Psi_{2j} \\ \vdots \\ \dot{e}_l = -\beta_1 e_l - \sum_{i=1, i\neq l}^{n} \theta_{il} e_i - \frac{1}{e_l} \left( \sum_{i=1, i\neq l}^{n} e_i \sum_{j=2}^{n} \Psi_{ij} \right) \\ \dot{e}_{l+1} = \sum_{k=1}^{n} \theta_{l+1,k} e_k + \sum_{j=2}^{n} \Psi_{l+1,j} \\ \vdots \\ \dot{e}_n = \sum_{k=1}^{n} \theta_{nk} e_k + \sum_{j=2}^{n} \Psi_{nj} \end{cases} \tag{38}$$

The following theorem presents the results for the synchronization of nonlinear systems described in (31) and (32) using a single control input $u_l$ applied to the $l$th state of the slave system dynamics.

**Theorem 2** *For the systems described in (31) and (32), for any $i = l$, the PI sliding surface selected as (35) along with a single sliding mode controller selected as*

$$u_l = -\sum_{k=1}^{n} \theta_{lk} e_k - \sum_{j=2}^{n} \Psi_{lj} - \beta_1 e_l - \sum_{i=1, i\neq l}^{n} \theta_{il} e_i - \frac{1}{e_l} \left( \sum_{i=1, i\neq l}^{n} e_i \sum_{j=2}^{n} \Psi_{ij} \right) - \sigma \, sign(s_l) \; ; \sigma > 0 \tag{39}$$

*associated with* $l$th *state of the slave system dynamics (32) is sufficient to ensure that the system trajectories converge to the sliding surface $s_l = 0$ and further, error trajectories converge to zero i.e. $\lim_{t\to\infty} \| e_i(t) \| \to 0$, for $i = 1, 2, 3, \ldots, n$; thus ensuring synchronization between the states of master system (31) and slave system (32).*

***Proof*** Consider a positive Lyapunov function candidate as follows:

$$V_7(\boldsymbol{e}) = 0.5 \sum_{i=1}^{n} e_i^2 \tag{40}$$

The time derivative of (40), while using equivalent sliding mode error dynamics (38) can be written as follows:

$$\dot{V}_7 = \sum_{i=1}^{n} e_i \dot{e}_i = e_l \dot{e}_l + \sum_{i=1, i\neq l}^{n} e_i \dot{e}_i$$

$$
\begin{aligned}
&= e_l\dot{e}_l + \sum_{i=1,\ i\neq l}^{n} e_i \left( \sum_{k=1}^{n} \theta_{ik} e_k + \sum_{j=2}^{n} \Psi_{ij} \right) \\
&= e_l\dot{e}_l + e_l \sum_{i=1,\ i\neq l}^{n} \theta_{il} e_i \\
&\quad + \sum_{i=1,\ i\neq l}^{n} e_i \sum_{k=1,\ k\neq l}^{n} \theta_{ik} e_k + \sum_{i=1,\ i\neq l}^{n} e_i \sum_{j=2}^{n} \Psi_{ij} \\
&= e_l \left( \dot{e}_l + \sum_{i=1,\ i\neq l}^{n} \theta_{il} e_i + \frac{1}{e_l} \left\{ \sum_{i=1,\ i\neq l}^{n} e_i \sum_{j=2}^{n} \Psi_{ij} \right\} \right) \\
&\quad + \sum_{i=1,\ i\neq l}^{n} e_i \sum_{k=1,\ k\neq l}^{n} \theta_{ik} e_k
\end{aligned}
$$

Using $\dot{e}_l$ from (37),$\dot{V}_7$ reduces to

$$
\dot{V}_7 = -\beta_1 e_l^2 + \sum_{i=1,\ i\neq l}^{n} e_i \sum_{k=1,\ k\neq l}^{n} \theta_{ik} e_k = -\boldsymbol{\zeta}^T P \boldsymbol{\zeta} \tag{41}
$$

where $\boldsymbol{\zeta} = \begin{bmatrix} e_1 & e_2 & \cdots & e_n \end{bmatrix}^T$ represents the state error vector and matrix $P$ is a real symmetric as described in (18).

With $\theta_{ii} < 0$, it can be stated that the zero equilibrium point ($e_1 = e_2 \cdots = e_n = 0$) of the system is globally asymptotically stable (GAS) if the real symmetric matrix $P$ is positive definite and Lyapunov function is radially bounded as $\dot{V}_7 \leq 0$ [62–64]. The above result holds as $P$ turns out to be positive definite while using assumption 1 and making suitable selection of design parameter $\beta_1 > 0$.

To establish the existence of sliding mode and convergence of system trajectories to it, consider a new Lyapunov function candidate as follows:

$$
V_8 = 0.5 s_l^2 \tag{42}
$$

The time derivative of (42), while using Eqs. (34) and (36) can be written as

$$
\begin{aligned}
\dot{V}_8 &= s_l \dot{s}_l \\
&= s_l \left( \dot{e}_l + \beta_1 e_l + \sum_{i=1,\ i\neq l}^{n} \theta_{il} e_i + \frac{1}{e_l} \left( \sum_{i=1,\ i\neq l}^{n} e_i \sum_{j=2}^{n} \Psi_{ij} \right) \right) \\
&= s_l \left( \sum_{k=1}^{n} \theta_{lk} e_k + \sum_{j=2}^{n} \Psi_{lj} + \beta_1 e_l + \sum_{i=1, i\neq l}^{n} \theta_{il} e_i \right. \\
&\quad \left. + \frac{1}{e_l} \left( \sum_{i=1, i\neq l}^{n} e_i \sum_{j=2}^{n} \Psi_{ij} \right) + u_l \right)
\end{aligned}
$$

Using the control function $u_l$ as given in (39), one can get

$$
\dot{V}_8 \leq -s_l \sigma sign\,(s_l) \leq -\sigma\,|s_l| \tag{43}
$$

As $\dot{V}_8 \leq 0$, thus, according to Lyapunov stability analysis, all the system trajectories converge to the sliding surface and the state dynamics in the sliding mode is asymptotically stable, which implies that $\lim_{t\to\infty} \|e_i\,(t)\| \to 0$, for $i = 1, 2, 3, \ldots, n$.

Thus, objective of synchronization of two systems of the proposed class in master–slave configuration is achieved.

## 4 SMC based synchronizing controller design with uncertain system parameters

In real-life situations, system parameters may be perturbed due to external disturbances and may not be known in advance. Hence, synchronization of chaotic systems with unknown system parameters is more important and realistic. For such a case, adaptation laws for uncertain parameters and corresponding control input is analytically derived here using SMC based synchronization scheme.

To address this problem, some parameters of the slave system which are in the range space of the controller are considered to be known and rest of the parameters are considered to be unknown. Let system (31) be considered as master system.

As earlier, assuming that the controller is applied to the $l$th state of the slave system, with parametric uncertainties, the slave system dynamics can be defined as follows:

$$
\dot{y}_i = \sum_{k=1}^{n} \hat{\theta}_{ik} y_k + \sum_{j=2}^{n} F'_{ij}; \quad i = 1, 2, 3, \ldots, n. \tag{44}
$$

where $\hat{\theta}_{ik}$ represents the uncertain coefficients associated with linear part of system dynamics which need to be estimated. The parametric errors between the parameter estimates and their true values can be defined as follows:

$$
\begin{aligned}
&\tilde{\theta}_{ik} = \hat{\theta}_{ik} - \theta_{ik}; \quad i, k = 1, 2, 3, \ldots, n; \quad i \neq l; \\
&\text{whereas } \hat{\theta}_{lk} = \theta_{lk} \text{for } i = l, \text{being known parameters.}
\end{aligned} \tag{45}
$$

Therefore, the dynamics of the slave system with controller applied to $l$th state of the system dynamics can be expressed as follows:

$$\begin{cases} \dot{y}_1 = \sum_{k=1}^{n} \hat{\theta}_{1k} y_k + \sum_{j=2}^{n} F'_{1j} \\ \dot{y}_2 = \sum_{k=1}^{n} \hat{\theta}_{2k} y_k + \sum_{j=2}^{n} F'_{2j} \\ \vdots \\ \dot{y}_l = \sum_{k=1}^{n} \theta_{lk} y_k + \sum_{j=2}^{n} F'_{lj} + u_l \\ \dot{y}_{l+1} = \sum_{k=1}^{n} \hat{\theta}_{l+1,k} y_k + \sum_{j=2}^{n} F'_{l+1,j} \\ \vdots \\ \dot{y}_n = \sum_{k=1}^{n} \hat{\theta}_{nk} y_k + \sum_{j=2}^{n} F'_{nj} \end{cases} \tag{46}$$

To achieve synchronization between master and slave system, the error between corresponding states is defined as follows:

$$e_i = y_i - x_i; \quad i = 1, 2, 3, \ldots, n \tag{47}$$

The resulting error dynamics using Eqs. (31), (45) and (46) can be written as follows:

$$\begin{cases} \dot{e}_1 = \sum_{k=1}^{n} \hat{\theta}_{1k} e_k + \sum_{k=1}^{n} \tilde{\theta}_{1k} x_k + \sum_{j=2}^{n} \Psi_{1j} \\ \dot{e}_2 = \sum_{k=1}^{n} \hat{\theta}_{2k} e_k + \sum_{k=1}^{n} \tilde{\theta}_{2k} x_k + \sum_{j=2}^{n} \Psi_{2j} \\ \vdots \\ \dot{e}_l = \sum_{k=1}^{n} \theta_{lk} e_k + \sum_{j=2}^{n} \Psi_{lj} + u_l \\ \dot{e}_{l+1} = \sum_{k=1}^{n} \hat{\theta}_{l+1,k} e_k + \sum_{k=1}^{n} \tilde{\theta}_{l+1,k} x_k + \sum_{j=2}^{n} \Psi_{l+1,j} \\ \vdots \\ \dot{e}_n = \sum_{k=1}^{n} \hat{\theta}_{nk} e_k + \sum_{k=1}^{n} \tilde{\theta}_{nk} x_k + \sum_{j=2}^{n} \Psi_{nj} \end{cases} \tag{48}$$

Here, nonlinear function $\Psi_{ij} = y_1 \left( -\sum_{j=2, j>i}^{n} e_j + \sum_{j=2, j<i}^{n} e_j \right) + e_1 \left( -\sum_{j=2, j>i}^{n} y_j + \sum_{j=2, j<i}^{n} y_j \right) + e_1 \left( \sum_{j=2, j>i}^{n} e_j - \sum_{j=2, j<i}^{n} e_j \right)$; for $i = 1, 2, 3, \ldots, n$.

In order to establish synchronization between master and the slave system, design of suitable SMC based controller and selection of proper adaptation laws for the unknown system parameters is necessary.

To ensure the asymptotic stability and synchronization operation, the proportional-integral switching surface $s_l$ in this case can be selected as follows:

$$s_l = e_l + \int_0^t \left\{ \beta_1 e_l + \frac{1}{e_l} \left( \sum_{i=1, i \neq l}^{n} e_i \sum\nolimits_{j=2}^{n} \Psi_{ij} \right) \right\} d\tau \tag{49}$$

here $\beta_1$ is a suitably selected positive constant. When the system operates in sliding mode, the following equation holds:

$$\dot{s}_l = \dot{e}_l + \beta_1 e_l + \frac{1}{e_l} \left( \sum_{i=1,\ i \neq l}^{n} e_i \sum_{j=2}^{n} \Psi_{ij} \right) = 0 \tag{50}$$

which implies that

$$\dot{e}_l = -\beta_1 e_l - \frac{1}{e_l} \left( \sum\nolimits_{i=1,\ i \neq l}^{n} e_i \sum_{j=2}^{n} \Psi_{ij} \right) \tag{51}$$

Therefore, from (48) and (51), the equivalent sliding mode dynamics can be written as follows:

$$\begin{cases} \dot{e}_1 = \sum_{k=1}^{n} \hat{\theta}_{1k} e_k + \sum_{k=1}^{n} \tilde{\theta}_{1k} x_k + \sum_{j=2}^{n} \Psi_{1j} \\ \dot{e}_2 = \sum_{k=1}^{n} \hat{\theta}_{2k} e_k + \sum_{k=1}^{n} \tilde{\theta}_{2k} x_k + \sum_{j=2}^{n} \Psi_{2j} \\ \vdots \\ \dot{e}_l = -\beta_1 e_l - \frac{1}{e_l} \left( \sum_{i=1,\ i \neq l}^{n} e_i \sum_{j=2}^{n} \Psi_{ij} \right) \\ \dot{e}_{l+1} = \sum_{k=1}^{n} \hat{\theta}_{l+1,k} e_k + \sum_{k=1}^{n} \tilde{\theta}_{l+1,k} x_k + \sum_{j=2}^{n} \Psi_{l+1,j} \\ \vdots \\ \dot{e}_n = \sum_{k=1}^{n} \hat{\theta}_{nk} e_k + \sum_{k=1}^{n} \tilde{\theta}_{nk} x_k + \sum_{j=2}^{n} \Psi_{nj} \end{cases} \tag{52}$$

**Theorem 3** *For the master system in (31) and the slave system with uncertain parameters $\hat{\theta}_{ik}$ for $i \neq l$ in (46), with PI sliding surface selected as (49), the following controller $u_l$ applied to the slave system (46), will ensure the occurrence of the sliding motion:*

$$u_l = -\beta_1 e_l - \sum_{k=1}^{n} \theta_{lk} e_k - \sum_{j=2}^{n} \Psi_{lj} - \frac{1}{e_l} \left\{ \sum_{i=1, i \neq l}^{n} e_i \sum_{j=2}^{n} \Psi_{ij} \right\} - \sigma sign\,(s_l)\,; \sigma > 0 \tag{53}$$

*Here, again $\beta_1 > 0$, is again suitably selected.*

*If the adaptation laws for uncertain system parameters are selected as follows:*

$$\dot{\tilde{\theta}}_{ik} = -\eta_i \tilde{\theta}_{ik} - \alpha_i x_k e_i - \alpha_i' e_k e_i; \quad \text{for } i,k = 1,2,3,\ldots,n; i \neq l. \tag{54}$$

*where* $\alpha_i = -sign\left(x_k e_i\right), \alpha_i' = -sign\left(e_k e_i\right)$ *and* $\eta_i > 0$ *are the constants governing the adaptation process of unknown system parameters, then the zero equilibrium point of the error dynamical system (52) is globally asymptotically stable (GAS) and the master and the slave systems in (31) and (46) are globally synchronized, for all initial conditions.*

***Proof*** To establish synchronization in uncertain environment for master system (31) and slave system (46), let the Lyapunov function be selected as

$$V_9\left(e_i, \tilde{\theta}_{ik}\right) = 0.5\left(\sum_{i=1}^{n} e_i^2\right) + 0.5\left(\sum_{i=1, i\neq l}^{n}\left(\sum_{k=1}^{n}\tilde{\theta}_{ik}^2\right)\right) \tag{55}$$

The time derivative of above Lyapunov function can be written as follows:

$$\begin{aligned}\dot{V}_9 &= \sum_{i=1}^{n} e_i\dot{e}_i + \sum_{i=1,\ i\neq l}^{n}\left(\sum_{k=1}^{n}\tilde{\theta}_{ik}\dot{\tilde{\theta}}_{ik}\right)\\ &= e_l\dot{e}_l + \sum_{i=1,\ i\neq l}^{n} e_i\dot{e}_i + \sum_{i=1,\ i\neq l}^{n}\left(\sum_{k=1}^{n}\tilde{\theta}_{ik}\dot{\tilde{\theta}}_{ik}\right)\end{aligned}$$

Using the error dynamics (52), one can get

$$\begin{aligned}\dot{V}_9 &= \left\{-\beta_1 e_l^2 - \left(\sum_{i=1,\ i\neq l}^{n} e_i \sum_{j=2}^{n}\Psi_{ij}\right)\right\}\\ &\quad + \sum_{i=1,\ i\neq l}^{n} e_i\left\{\sum_{k=1}^{n}\hat{\theta}_{ik}e_k + \sum_{k=1}^{n}\tilde{\theta}_{ik}x_k\right.\\ &\quad \left. + \sum_{j=2}^{n}\Psi_{ij}\right\} + \sum_{i=1,i\neq l}^{n}\left(\sum_{k=1}^{n}\tilde{\theta}_{ik}\dot{\tilde{\theta}}_{ik}\right)\\ &= \left\{-\beta_1 e_l^2 + \sum_{i=1}^{n} e_i \sum_{k=1,\ k\neq l}^{n}\theta_{ik}e_k\right\}\\ &\quad + \sum_{i=1,\ i\neq l}^{n} e_i\left(\sum_{k=1}^{n}\tilde{\theta}_{ik}e_k\right)\\ &\quad + \sum_{i=1,\ i\neq l}^{n} e_i\left(\sum_{k=1}^{n}\tilde{\theta}_{ik}x_k\right)\\ &\quad + \sum_{i=1,\ i\neq l}^{n}\left(\sum_{k=1}^{n}\tilde{\theta}_{ik}\dot{\tilde{\theta}}_{ik}\right)\end{aligned}$$

$$\begin{aligned}&= -\boldsymbol{\zeta}^T P'\boldsymbol{\zeta} + \sum_{i=1,\ i\neq l}^{n} e_i\left(\sum_{k=1}^{n}\tilde{\theta}_{ik}e_k\right)\\ &\quad + \sum_{i=1,\ i\neq l}^{n} e_i\left(\sum_{k=1}^{n}\tilde{\theta}_{ik}x_k\right)\\ &\quad + \sum_{i=1}^{n}\left(\sum_{k=1}^{n}\tilde{\theta}_{ik}\dot{\tilde{\theta}}_{ik}\right)\end{aligned}$$

For $i = 1,2,3,\ldots,n; i \neq l$, $\dot{V}_9$ can be expanded as follows:

$$\begin{aligned}\dot{V}_9 &= -\boldsymbol{\zeta}^T P'\boldsymbol{\zeta} + \sum_{k=1}^{n}\left(\tilde{\theta}_{1k}x_k e_1 + \tilde{\theta}_{1k}e_k e_1 + \tilde{\theta}_{1k}\dot{\tilde{\theta}}_{1k}\right)\\ &\quad + \sum_{k=1}^{n}\left(\tilde{\theta}_{2k}x_k e_2 + \tilde{\theta}_{2k}e_k e_2 + \tilde{\theta}_{2k}\dot{\tilde{\theta}}_{2k}\right) + \ldots\\ &\quad + \sum_{k=1}^{n}\left(\tilde{\theta}_{nk}x_k e_n + \tilde{\theta}_{nk}e_k e_n + \tilde{\theta}_{nk}\dot{\tilde{\theta}}_{nk}\right)\end{aligned}$$

with the proper selection of adaptation laws as per (54), $\dot{V}_9$ becomes

$$\begin{aligned}\dot{V}_9 &= -\boldsymbol{\zeta}^T P'\boldsymbol{\zeta} - \sum_{k=1}^{n}\eta_1\tilde{\theta}_{1k}^2\\ &\quad - \sum_{k=1}^{n}\eta_2\tilde{\theta}_{2k}^2 - \ldots - \sum_{k=1}^{n}\eta_n\tilde{\theta}_{nk}^2\end{aligned} \tag{56}$$

Here, $\boldsymbol{\zeta} = \begin{bmatrix} e_1 & e_2 & \cdots & e_n \end{bmatrix}^T$ is the state error vector similar to earlier case and $P'$ is a real symmetric matrix and can be expressed as

$$P' = \begin{vmatrix} -\theta_{11} & \frac{(\theta_{12}+\theta_{21})}{2} & \ldots & \frac{(\theta_{1l}+\theta_{l1})}{2} & \ldots & \frac{(\theta_{1n}+\theta_{n1})}{2} \\ \frac{(\theta_{21}+\theta_{12})}{2} & -\theta_{22} & \ldots & \frac{(\theta_{2l}+\theta_{l2})}{2} & \ldots & \frac{(\theta_{2n}+\theta_{n2})}{2} \\ \vdots & \vdots & \vdots & \vdots & \vdots & \vdots \\ \frac{(\theta_{l1}+\theta_{1l})}{2} & \frac{(\theta_{l2}+\theta_{2l})}{2} & \ldots & \beta_1 & \ldots & \frac{(\theta_{ln}+\theta_{nl})}{2} \\ \vdots & \vdots & \vdots & \vdots & \vdots & \vdots \\ \frac{(\theta_{n1}+\theta_{1n})}{2} & \frac{(\theta_{n2}+\theta_{2n})}{2} & \ldots & \frac{(\theta_{nl}+\theta_{ln})}{2} & \ldots & -\theta_{nn} \end{vmatrix}. \tag{57}$$

Using adaptation laws given in (54) and with all negative diagonal entries of the system matrix $A$, it can be shown that the zero equilibrium point ($e_1 = e_2 = \ldots = e_n = 0$) of the error dynamical system is globally asymptotically stable (GAS) as $\dot{V}_9 \leq 0$ if the real symmetric matrix $P'$ is positive definite [62–64]. Therefore by using Sylvester's theorem all

principal minors of $P'$ must be positive, which implies that the following conditions should be satisfied:

$$\begin{cases} i. & P'_{11} = -\theta_{11} > 0 \\ ii. & P'_{22} = \left\{\theta_{11}\theta_{22} - \frac{(\theta_{21}+\theta_{12})^2}{4}\right\} > 0 \\ & \vdots \\ iii. & P'_{nn} = \begin{vmatrix} -\theta_{11} & \frac{(\theta_{12}+\theta_{21})}{2} & \dots & \frac{(\theta_{1l}+\theta_{l1})}{2} & \dots & \frac{(\theta_{1n}+\theta_{n1})}{2} \\ \frac{(\theta_{21}+\theta_{12})}{2} & -\theta_{22} & \dots & \frac{(\theta_{2l}+\theta_{l2})}{2} & \dots & \frac{(\theta_{2n}+\theta_{n2})}{2} \\ \vdots & \vdots & \vdots & \vdots & \vdots & \vdots \\ \frac{(\theta_{l1}+\theta_{1l})}{2} & \frac{(\theta_{l2}+\theta_{2l})}{2} & \dots & \beta_1 & \dots & \frac{(\theta_{ln}+\theta_{nl})}{2} \\ \vdots & \vdots & \vdots & \vdots & \vdots & \vdots \\ \frac{(\theta_{n1}+\theta_{1n})}{2} & \frac{(\theta_{n2}+\theta_{2n})}{2} & \dots & \frac{(\theta_{nl}+\theta_{ln})}{2} & \dots & -\theta_{nn} \end{vmatrix} > 0 \end{cases} \tag{58}$$

To ensure convergence of system trajectories to the sliding surface and to establish synchronization between master and the slave system given in (31) and (46), if the controller $u_l$ in (53) is applied in the $l$th state of the slave system (46), then the master and the slave system trajectories converge to each other, ensuring that $\lim_{t\to\infty} \|e_i\| \to 0$, for $i = 1, 2, 3, \dots, n$.

In order to prove this, new Lyapunov function is selected as

$$V_{10} = 0.5 s_l^2 \tag{59}$$

The time derivative of $V_{10}$, while using (48) and (50), gives

$$\begin{aligned} \dot{V}_{10} &= s_l \dot{s}_l \\ &= s_l \left[ \dot{e}_l + \beta_1 e_l + \frac{1}{e_l} \left( \sum_{i=1,\ i\neq l}^{n} e_i \sum_{j=2}^{n} \Psi_{ij} \right) \right] \\ &= s_l \left[ \sum_{k=1}^{n} \theta_{lk} e_k + \sum_{j=2}^{n} \Psi_{lj} \right. \\ &\quad \left. + \beta_1 e_l + \frac{1}{e_l} \left( \sum_{i=1, i\neq l}^{n} e_i \sum_{j=2}^{n} \Psi_{ij} \right) + u_l \right] \end{aligned}$$

Using the control function $u_l$ from (53), $\dot{V}_{10}$ becomes

$$\Longrightarrow \dot{V}_{10} = -\sigma s_l sign\,(s_l) \leq -\sigma\,|s_l| \tag{60}$$

Therefore it can be concluded that the zero equilibrium point ($e_1 = e_2 \cdots = e_n = 0$) is globally asymptotically stable (GAS) as Lyapunov function is radially bounded and the master and slave systems are globally synchronized with each other. □

***Remark 4*** To establish synchronization between master system (31) and slave system (46), the parameters of the systems belonging to proposed class should be such that suitable selection of feedback gain $\beta_1$ is possible to ensure that conditions in (58) are satisfied, thus, leading the error dynamical system (52) to be globally asymptotically stable.

***Remark 5*** In case if the description of the nonlinearity differs from as described in Eq. (9), then, associating additional control function with the equation having such nonlinearity and following the proposed procedure, the stabilization and synchronization results can be paralley derived.

## 5 Numerical example

To analyze the proposed strategy, example of hyperchaotic Lorenz–Stenflo system belonging to the class described in (8) is considered. Lennart Stenflo, studied the equations governing the atmospheric waves in 1996. Based on low-frequency and short-wavelength approximations, he was able to derive a set of simplified equations. Then, using same strategy, he constructed the Lorenz–Stenflo (LS) system [59]. With parameter values of $a = 1, b = 0.7, c = 26, d = 1.5$, Lorenz–Stenflo (LS) system can be described by a set of nonlinear differential equations as follows:

$$\begin{cases} \dot{x}_1 = a\,(x_2 - x_1) + d x_4 \\ \dot{x}_2 = x_1\,(c - x_3) - x_2 \\ \dot{x}_3 = x_1 x_2 - b x_3 \\ \dot{x}_4 = -x_1 - a x_4 \end{cases} \tag{61}$$

The famous Lorenz system and LS system share the same basic foundation. The LS system is similar to the Lorenz system, but with addition of new control parameter $d$ and the new state variable $x_4$. For the initial conditions taken as $\boldsymbol{x}\,(0) = \begin{bmatrix} 2 & 4 & 6 & 8 \end{bmatrix}^T$ and simulations run for 100 s, three-dimensional phase portraits are depicted in Fig. 2a–d.

### 5.1 Switching surface and stabilizing controller design

To analyze the problem of stabilization discussed in Sect. 2, controlled dynamics of the Lorenz–Stenflo system can be considered as follows:

$$\begin{cases} \dot{x}_1 = a\,(x_2 - x_1) + d x_4 + u_1 \\ \dot{x}_2 = x_1\,(c - x_3) - x_2 \\ \dot{x}_3 = x_1 x_2 - b x_3 \\ \dot{x}_4 = -x_1 - a x_4 \end{cases} \tag{62}$$

where $u_1$ is the control input to be designed for stabilizing the above system.

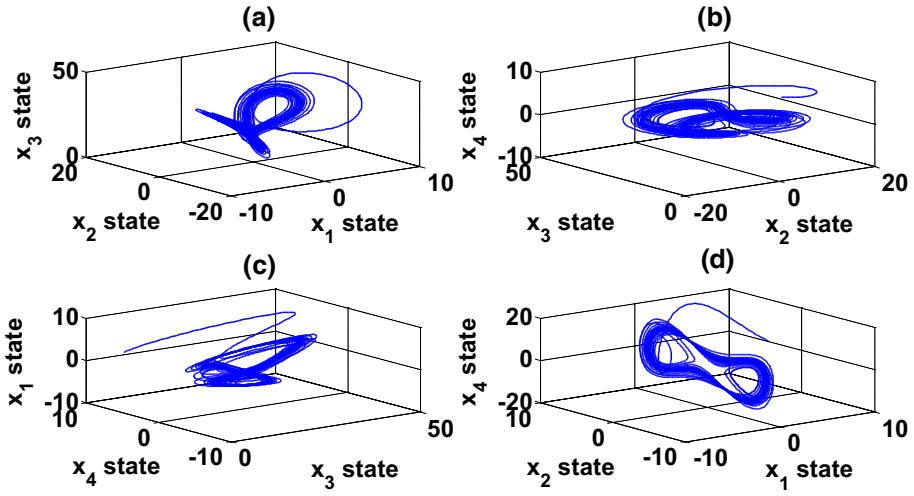


**Fig. 2** The phase portraits of hyperchaotic Lorenz–Stenflo system: **a**–**d** three dimensional phase portrait for different states

In sliding mode control based stabilization approach, selection of appropriate switching surface is done which guarantees the stability of equivalent dynamics in sliding mode so that the state dynamics converges to zero. Thereafter, a sliding mode control law is established which guarantees the existence of sliding mode $s_1 = 0$.

From the controlled dynamics of L–S system in (62) and sliding surface in (10), $n = 4, l = 1, \sum_{j=2}^{4} F_{1j} = \sum_{j=2}^{4} F_{4j} = 0, \sum_{j=2}^{4} F_{2j} = -x_1x_3$ and $\sum_{j=2}^{4} F_{3j} = x_1x_2$. Further, from (9) and (61), the system matrix can be written as follows:

$$A = \begin{bmatrix} \theta_{11} & \theta_{12} & \theta_{13} & \theta_{14} \\ \theta_{21} & \theta_{22} & \theta_{23} & \theta_{24} \\ \theta_{31} & \theta_{32} & \theta_{33} & \theta_{34} \\ \theta_{41} & \theta_{42} & \theta_{43} & \theta_{44} \end{bmatrix} = \begin{bmatrix} -a & a & 0 & d \\ c & -1 & 0 & 0 \\ 0 & 0 & -b & 0 \\ -1 & 0 & 0 & -a \end{bmatrix} \tag{63}$$

Therefore, the switching function as per Eq. (10) can be written as follows:

$$s_1 = x_1 + \int_0^t (\beta_1 x_1 + cx_2 - x_4)\, d\tau \tag{64}$$

where $\beta_1$ is the positive constant specified by the designer. As per Utkin [61], in sliding mode, the following equation holds:

$$\dot{s}_1 = 0 \tag{65}$$

Therefore, from (64) and (65), the sliding mode dynamics can be written as

$$\dot{s}_1 = \dot{x}_1 + \beta_1 x_1 + cx_2 - x_4 = 0 \tag{66}$$

From (66), one can write

$$\dot{x}_1 = -\beta_1 x_1 - cx_2 + x_4 \tag{67}$$

Therefore, from (62) and (67), the equivalent sliding mode dynamics for the system (62) can be written as follows:

$$\begin{cases} \dot{x}_1 = -\beta_1 x_1 - cx_2 + x_4 \\ \dot{x}_2 = x_1 (c - x_3) - x_2 \\ \dot{x}_3 = x_1 x_2 - bx_3 \\ \dot{x}_4 = -x_1 - ax_4 \end{cases} \tag{68}$$

To analyze the stability of sliding mode dynamics in (68), the Lyapunov function candidate in (16) becomes as follows:

$$V_3 = 0.5 \left( x_1^2 + x_2^2 + x_3^2 + x_4^2 \right) \tag{69}$$

Time derivative of above Lyapunov function can be written as

$$\dot{V}_3 = x_1\dot{x}_1 + x_2\dot{x}_2 + x_3\dot{x}_3 + x_4\dot{x}_4 \tag{70}$$

Using the equivalent sliding mode dynamics (68) in (70), $\dot{V}_3$ becomes

$$\begin{aligned} \dot{V}_3 &= -\beta_1 x_1^2 - x_2^2 - bx_3^2 - ax_4^2 \\ &= -\begin{bmatrix} x_1 & x_2 & x_3 & x_4 \end{bmatrix} \begin{bmatrix} \beta_1 & 0 & 0 & 0 \\ 0 & 1 & 0 & 0 \\ 0 & 0 & b & 0 \\ 0 & 0 & 0 & a \end{bmatrix} \begin{bmatrix} x_1 \\ x_2 \\ x_3 \\ x_4 \end{bmatrix} = -\boldsymbol{x}^T P \boldsymbol{x} \end{aligned}$$

$\Rightarrow \dot{V}_3 \leq 0.$

here $\beta_1 > 0$ and $P = \begin{bmatrix} \beta_1 & 0 & 0 & 0 \\ 0 & 1 & 0 & 0 \\ 0 & 0 & b & 0 \\ 0 & 0 & 0 & a \end{bmatrix}$ which is clearly positive definite.

Therefore, according to Lyapunov stability theory, the sliding motion on the sliding manifold is stable and $\lim_{t\to\infty} \|x_i\| \to 0$, for $i = 1, 2, 3, 4$.

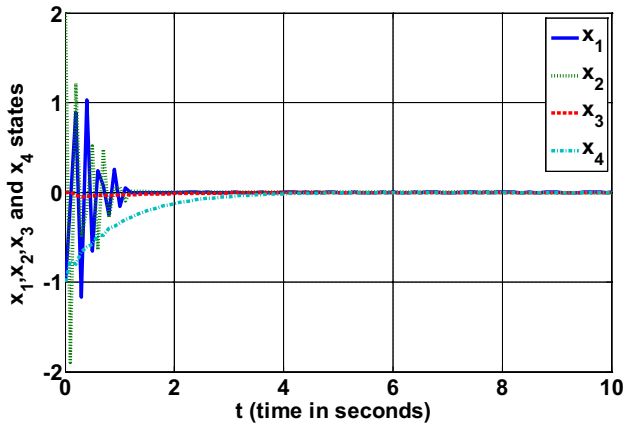


**Fig. 3** Variation of system states with time showing stabilization behaviour

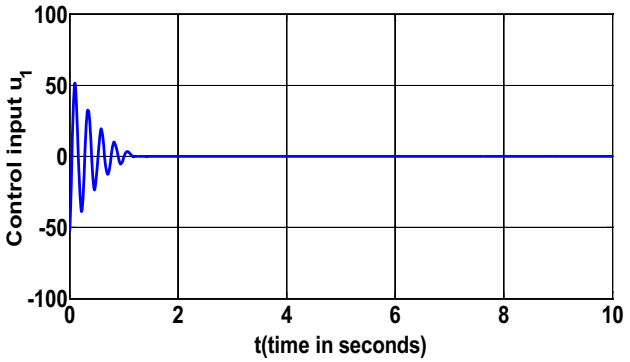


**Fig. 4** Variation of control input $u_1$ in Eq. (71) with time

Now, next step is to design SMC based controller so that system trajectories are directed on to the sliding surface $s_1 = 0$.

Based on Theorem 1 and Eq. (15), the sliding mode controller can be written as follows:

$$u_1 = -(\beta_1 - a)\, x_1 - (a + c)\, x_2 - (d - 1)\, x_4 - \sigma sign(s_1)\,; \sigma > 0 \quad (71)$$

The controller $u_1$ in (71) makes the time derivative of Lyapunov function (19) as negative definite i.e. $\dot{V}_4 \leq -\sigma|s_1| \leq 0$.

As $\dot{V}_4 \leq 0$, implies that all the system trajectories converge to the sliding surface and the state dynamics in the sliding mode is asymptotically stable i.e. $\lim_{t\to\infty} \|x_i\|(t) \to 0$, for $i = 1, 2, 3, 4$.

Detailed simulation results depicting the convergence behaviour of the system states and variation of control input $u_1$ with respect to time are presented in Figs. 3 and 4 in Sect. 6.

## 5.2 Switching surface and synchronizing controller design

To analyze synchronization operation in master–slave configuration, system (61) is considered as master system. Similarly, the controlled dynamics of the slave system can be written as follows:

$$\begin{cases} \dot{y}_1 = a\,(y_2 - y_1) + d y_4 + u_1 \\ \dot{y}_2 = y_1\,(c - y_3) - y_2 \\ \dot{y}_3 = y_1 y_2 - b y_3 \\ \dot{y}_4 = -y_1 - a y_4 \end{cases} \quad (72)$$

where $u_1$ is the control input to be designed for synchronizing the system (61) and (72).

In order to achieve synchronization between master and the slave system described in (61) and (72), respectively, the error between the corresponding states of the master and the slave systems can be defined as follows:

$e_i = y_i - x_i$; for $i = 1, 2, 3, 4$.

Therefore, the resulting error dynamics from (61) and (72) can be written as follows:

$$\begin{cases} \dot{e}_1 = -a e_1 + a e_2 + d e_4 + u_1 \\ \dot{e}_2 = c e_1 - e_2 - y_1 e_3 - y_3 e_1 + e_1 e_3 \\ \dot{e}_3 = -a e_3 + y_1 e_2 + y_2 e_1 - e_1 e_2 \\ \dot{e}_4 = -e_1 - a e_4 \end{cases} \quad (73)$$

In this case, $n = 4, l = 1, \sum_{j=2}^{4} \Psi_{1j} = \sum_{j=2}^{4} \Psi_{4j} = 0, \sum_{j=2}^{4} \Psi_{2j} = -y_1 e_3 - y_3 e_1 - e_1 e_3, \sum_{j=2}^{4} \Psi_{3j} = y_1 e_2 + y_2 e_1 - e_1 e_2$ and the system matrix $A$ is the same as described in (63).

To achieve synchronization, from (35), the proportional-integral (PI) switching surface $s_1$ can be written as

$$s_1 = e_1 + \int_0^t (\beta_1 e_1 + c e_2 - y_3 e_2 + y_2 e_3 - e_4)\, d\tau \quad (74)$$

where $\beta_1 > 0$ is a constant specified by the designer. When system operates in sliding mode the following equation holds:

$$\dot{s}_1 = 0 \quad (75)$$

Therefore from (74) and (75), the sliding mode dynamics can be obtained as

$$\dot{s}_1 = \dot{e}_1 + \beta_1 e_1 + c e_2 - y_3 e_2 + y_2 e_3 - e_4 = 0 \quad (76)$$

From (75) and (76), $\dot{e}_1$ can be written as follows:

$$\dot{e}_1 = -\beta_1 e_1 - c e_2 + y_3 e_2 - y_2 e_3 + e_4 \quad (77)$$

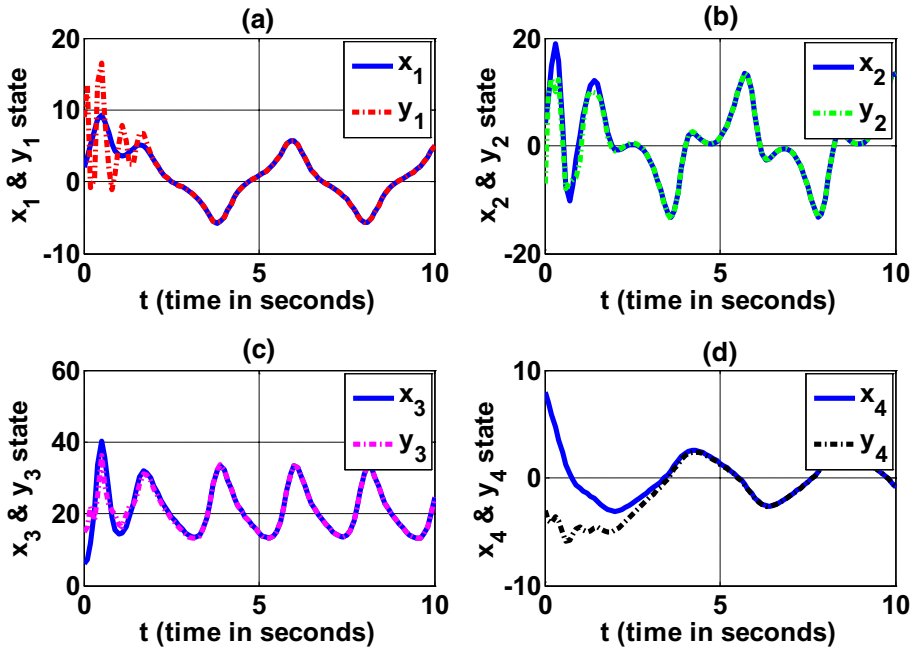


**Fig. 5** Response of Lorenz–Stenflo system: **a**–**d** synchronization behaviour of master and slave system states with controller (81)

Hence, from (73) and (77), the equivalent sliding mode dynamics for the error dynamics can be written as follows:

$$\begin{cases} \dot{e}_1 = -\beta_1 e_1 - c e_2 + y_3 e_2 - y_2 e_3 + e_4 \\ \dot{e}_2 = c e_1 - e_2 - y_1 e_3 - y_3 e_1 + e_1 e_3 \\ \dot{e}_3 = -a e_3 + y_1 e_2 + y_2 e_1 - e_1 e_2 \\ \dot{e}_4 = -e_1 - a e_4 \end{cases} \tag{78}$$

In order to analyze the stability of the above equivalent sliding mode dynamics, the Lyapunov function in (40) becomes

$$V_7 = 0.5\left(e_1^2 + e_2^2 + e_3^2 + e_4^2\right) \tag{79}$$

Time derivative of the above Lyapunov function can be written as follows:

$$\dot{V}_7 = e_1\dot{e}_1 + e_2\dot{e}_2 + e_3\dot{e}_3 + e_4\dot{e}_4 \tag{80}$$

Using the equivalent sliding mode dynamics (78) in (80), $\dot{V}_7$ becomes

$$\begin{aligned} \dot{V}_7 &= -\beta_1 e_1^2 - e_2^2 - b e_3^2 - a e_4^2 \\ &= -\begin{bmatrix} e_1 & e_2 & e_3 & e_4 \end{bmatrix} \begin{bmatrix} \beta_1 & 0 & 0 & 0 \\ 0 & 1 & 0 & 0 \\ 0 & 0 & b & 0 \\ 0 & 0 & 0 & a \end{bmatrix} \begin{bmatrix} e_1 \\ e_2 \\ e_3 \\ e_4 \end{bmatrix} = -e^T P e \end{aligned}$$

$$\Rightarrow \dot{V}_7 \leq 0$$

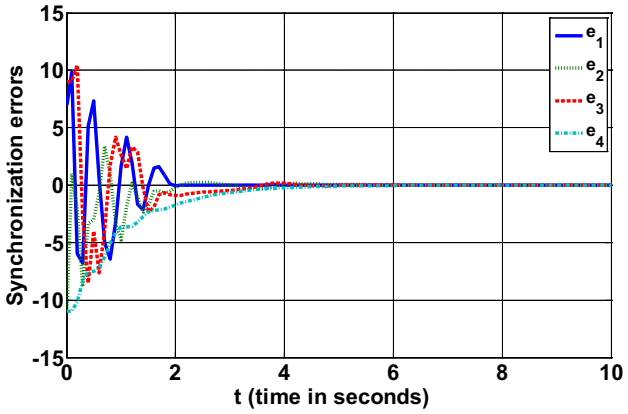


**Fig. 6** Convergence of synchronization errors between the states of the master and the slave systems

here $\beta_1 > 0$ and $P = \begin{bmatrix} \beta_1 & 0 & 0 & 0 \\ 0 & 1 & 0 & 0 \\ 0 & 0 & b & 0 \\ 0 & 0 & 0 & a \end{bmatrix}$ which is clearly positive definite.

Therefore, according to Lyapunov stability analysis, the sliding motion on the sliding surface is stable and $\lim_{t\to\infty} \|e_i\|(t) \to 0$, for $i = 1, 2, 3, 4$.

Based on Theorem 2 and Eq. (39), the controller $u_1$ can be accordingly written so that system trajectories are directed towards the sliding surface as follows:

$$\begin{aligned} u_1 = &-(k-a)e_1 - (a+c)e_2 - (d-1)e_4 + y_3 e_2 - y_2 e_3 \\ &-\sigma\, sign(s_1);\ \sigma > 0 \end{aligned} \tag{81}$$

The controller $u_1$ in (81) makes the time derivative of Lyapunov function (42) as negative definite i.e. $\dot{V}_8 \leq -\sigma|s_1| \leq 0$.

As $\dot{V}_8 \leq 0$, implies that all system trajectories converge to sliding surface and the state dynamics in the sliding mode is asymptotically stable i.e. $\lim_{t\to\infty} \|e_i(t)\| \to 0$, for $i = 1, 2, 3, 4$. Detailed simulations results are shown in Figs. 5, 6 and 7 in Sect. 6, where synchronization behaviour of corresponding states of the master and the slave systems, the convergence behaviour of the synchronization errors and variation of control input with respect to time are presented.

### 5.3 Switching surface and synchronizing controller design with uncertain system parameters

To analyze the synchronization operation with uncertain system parameters, it is assumed that the master system parameters are completely known. Further, it is assumed that the parameters of the slave system which are in the range space of the sliding mode controller are known and rest of the parameters are unknown. Again, system described in (61) is considered as the master system.

The dynamics of the slave system with parametric uncertainties can be redefined as follows:

$$\begin{cases} \dot{y}_1 = a(y_2 - y_1) + dy_4 + u_1 \\ \dot{y}_2 = y_1(\hat{c} - y_3) - y_2 \\ \dot{y}_3 = y_1 y_2 - \hat{b} y_3 \\ \dot{y}_4 = -y_1 - a y_4 \end{cases} \tag{82}$$

where $\hat{b}$ and $\hat{c}$ are the uncertain slave system parameters and need to be estimated. The parameters $a$ and $d$ are assumed to be completely known. Here, objective is to design a sliding mode controller and to determine suitable adaptation laws for the uncertain system parameters in order to establish synchronization between system (61) and (82). To meet out this objective, the error dynamical system between master system (61) and slave system (82) can be written as follows:

$$\begin{cases} \dot{e}_1 = -ae_1 + ae_2 + de_4 + u_1 \\ \dot{e}_2 = \hat{c}e_1 - e_2 - y_1e_3 - y_3e_1 + e_1e_3 + \tilde{c}x_1 \\ \dot{e}_3 = -\hat{b}e_3 + y_1e_2 + y_2e_1 - e_1e_2 - \tilde{b}x_3 \\ \dot{e}_4 = -e_1 - ae_4 \end{cases} \tag{83}$$

where, $\tilde{b} = \hat{b} - b$ and $\tilde{c} = \hat{c} - c$ are defined to be parametric errors between parameter estimates and their true values.

Analysis of the switching surface and design of sliding mode controller can be done by applying the results derived in Sect. 4. As earlier, here, $n = 4, l = 1, \sum_{j=2}^{4} \Psi_{1j} = \sum_{j=2}^{4} \Psi_{4j} = 0, \sum_{j=2}^{4} \Psi_{2j} = -y_1e_3 - y_3e_1 - e_1e_3, \sum_{j=2}^{4} \Psi_{3j} = y_1e_2 + y_2e_1 - e_1e_2$.

For ensuring the asymptotic stability, the proportional-integral switching surface from (49) can be written as follows:

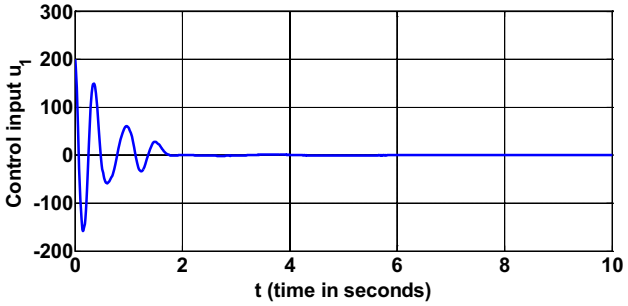


**Fig. 7** Variation of control input $u_1$ in Eq. (81) with time

$$s_1 = e_1 + \int_0^t \{\beta_1 e_1 - y_3e_2 + y_2e_3\} d\tau \tag{84}$$

where $\beta_1 > 0$ is a positive constant suitably selected by the designer.

As earlier, when system operates in sliding mode, the following Utkin condition [61] holds:

$$\dot{s}_1 = \dot{e}_1 + \beta_1 e_1 - y_3e_2 + y_2e_3 = 0 \tag{85}$$

Therefore, the above dynamics can be written as follows:

$$\dot{e}_1 = -\beta_1 e_1 + y_3e_2 - y_2e_3 \tag{86}$$

Hence, from (83) and (86), the equivalent sliding mode dynamics can be written as

$$\begin{cases} \dot{e}_1 = -\beta_1 e_1 + y_3e_2 - y_2e_3 \\ \dot{e}_2 = \hat{c}e_1 - e_2 - y_1e_3 - y_3e_1 + e_1e_3 + \tilde{c}x_1 \\ \dot{e}_3 = -\hat{b}e_3 + y_1e_2 + y_2e_1 - e_1e_2 - \tilde{b}x_3 \\ \dot{e}_4 = -e_1 - ae_4 \end{cases} \tag{87}$$

In order to analyze the stability of above equivalent sliding mode dynamics, the Lyapunov function (55) becomes

$$V_9 = 0.5\left[e_1^2 + e_2^2 + e_3^2 + e_4^2 + \tilde{b}^2 + \tilde{c}^2\right]$$

Time derivative of above Lyapunov function becomes

$$\dot{V}_9 = e_1\dot{e}_1 + e_2\dot{e}_2 + e_3\dot{e}_3 + e_4\dot{e}_4 + \tilde{b}\dot{\tilde{b}} + \tilde{c}\dot{\tilde{c}}$$

Using equivalent error dynamics given in (87), the above expression becomes

$$\dot{V}_9 = -\beta_1 e_1^2 - e_2^2 - be_3^2 - ae_4^2 + ce_1e_2 - e_1e_4 + \tilde{b}\left(\dot{\tilde{b}} - e_3^2 - e_3x_3\right) + \tilde{c}\left(\dot{\tilde{c}} + e_1e_2 + e_2x_1\right)$$

Based on Theorem 3 and Eq. (54), following selection of adaptation laws for uncertain system parameters can be made:

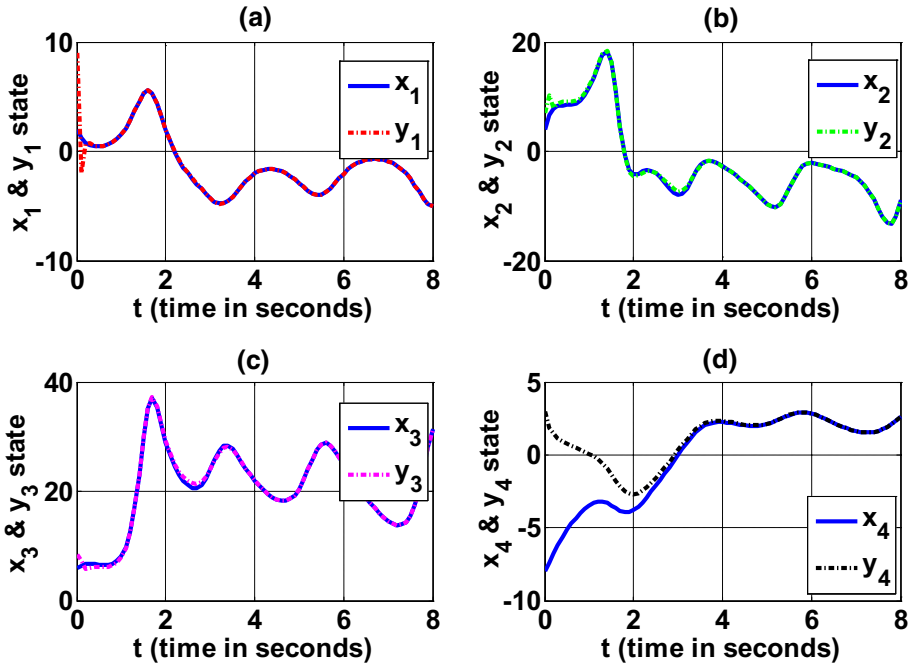


**Fig. 8** Response of Lorenz–Stenflo system: **a**–**d** synchronization behaviour of master and slave system states with uncertain system parameters

$$\begin{cases} \dot{\tilde{b}} = \dot{\hat{b}} = -\eta_1 \tilde{b} + x_3 e_3 + e_3^2; \eta_1 > 0 \\ \dot{\tilde{c}} = \dot{\hat{c}} = -\eta_2 \tilde{c} - e_2 x_1 - e_1 e_2; \eta_2 > 0 \end{cases} \tag{88}$$

Using above adaptive laws, $\dot{V}_9$ becomes

$$\begin{aligned} \dot{V}_9 &= -\beta_1 e_1^2 - e_2^2 - b e_3^2 - a e_4^2 + c e_1 e_2 \\ &\quad - e_1 e_4 - \eta_1 \tilde{b}^2 - \eta_2 \tilde{c}^2 \\ &= -\boldsymbol{\zeta}^T P' \boldsymbol{\zeta} - \eta_1 \tilde{b}^2 - \eta_2 \tilde{c}^2 \end{aligned} \tag{89}$$

where $\boldsymbol{\zeta} = \left[\, |e_1| \;\; |e_2| \;\; |e_3| \;\; |e_n| \,\right]^T$ is the absolute error vector. From (57) and (89), the real symmetric matrix $P'$ can be expressed as

$$P' = \begin{bmatrix} \beta_1 & -\frac{c}{2} & 0 & \frac{1}{2} \\ -\frac{c}{2} & 1 & 0 & 0 \\ 0 & 0 & b & 0 \\ \frac{1}{2} & 0 & 0 & a \end{bmatrix} \tag{90}$$

The zero equilibrium point of the error dynamical system is globally asymptotically stable (GAS) if the real symmetric matrix $P'$ is positive definite. Therefore, based on Sylvester's theorem, the following conditions must be satisfied:

$$\begin{cases} i. \quad \beta_1 > 0 \\ ii. \quad \beta_1 > \frac{c^2}{4} \\ iii. \; \beta_1 > \frac{c^2}{4} + \frac{1}{4a} \end{cases} \tag{91}$$

Hence, it can be clearly seen that with the proper choice of feedback gain $\beta_1$, the real symmetric matrix $P'$ will be positive definite and $\dot{V}_9$ becomes negative definite i.e. $\dot{V}_9 \leq 0$ and the zero equilibrium point of error dynamical system (87) is globally asymptotically stable.

From Theorem 3 and Eq. (53), the controller $u_1$ can be accordingly written as follows:

$$u_1 = -(\beta_1 - a)\, e_1 - (a - y_3)\, e_2 - d e_4 - y_2 e_3 - \sigma\, sign\,(s_1) \tag{92}$$

The choice of above controller makes the time derivative of Lyapunov function $V_{10}$ in (59) as negative definite i.e.

$$\dot{V}_{10} \leq -\sigma |s_1| \leq 0. \tag{93}$$

As $\dot{V}_{10} \leq 0$, means that all trajectories of the systems in (61) and (82) converge to sliding surface $s_1$ in (84) and the error dynamics in sliding mode is asymptotically stable i.e. $\lim_{t \to \infty} \| e_i\,(t) \| \to 0$, for $i = 1, 2, 3, 4$.

Detailed simulation results are presented in Sect. 6, where synchronization behaviour of corresponding states of the master and the slave systems and the convergence of synchronization errors along with the convergence of uncertain system parameters to their true values is depicted.

***Remark 6*** Some of the entries of the system matrix $A$ in (63) may be exactly known as they are not linked to the actual system parameters. For such entries $\theta_{ij}$, the uncertainty is not required to be considered. For example, in the system dynamics of Lorenz–Stenflo system $\theta_{22} = -1$, hence, uncertainty in $\theta_{22}$ for Lorenz–Stenflo system is not considered.

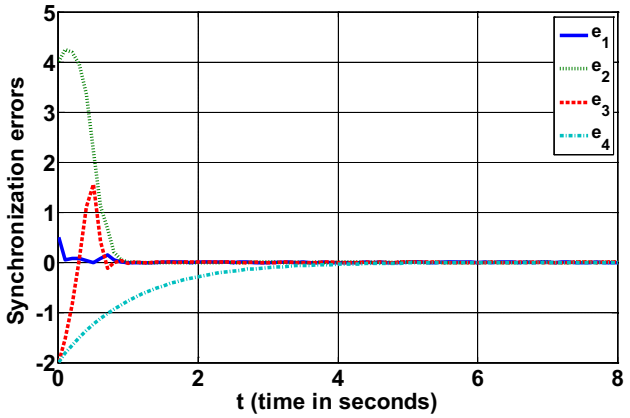


**Fig. 9** Convergence of synchronization errors between the states of the master and the slave systems

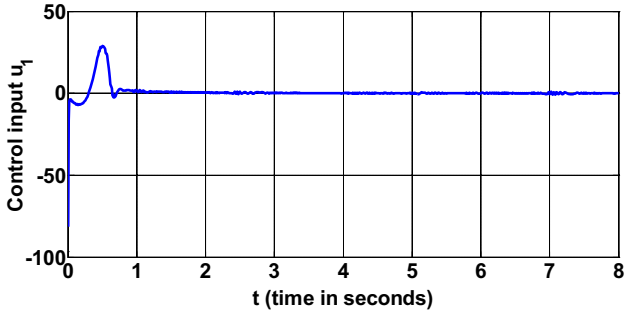


**Fig. 10** Variation of control input $u_1$ in Eq. (92) with time in case of uncertain system parameters

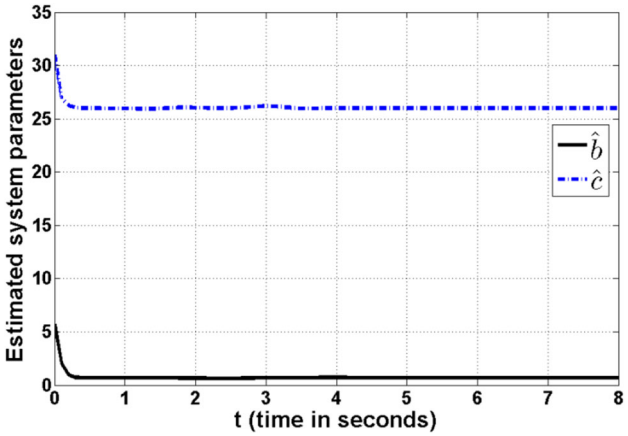


**Fig. 11** Convergence of estimates of uncertain system parameters to their true values

## 6 Numerical simulations

In this section, numerical simulations are presented to illustrate the effectiveness of the proposed approach. To validate the results derived in Sect. 2, example of fourth order Lorenz–Stenflo hyperchaotic system is considered. The fourth-order Runge–Kutta method is used to solve the nonlinear system with step size of 0.01. For the purpose of simulations, the system parameters are taken as $a = 1, b = 0.7, c = 26, d = 1.5$ and $\sigma > 0$ has to be suitably selected. For the case of stabilization, the initial conditions are taken as $x(0) = \begin{bmatrix} 2 & 4 & 6 & 8 \end{bmatrix}^T$ and the control gain is selected as $\beta_1 = 2$. Figure 3 presents the time response of various state variables depicting the stabilization results with the proposed sliding mode controller in (71). These simulations are run for 10 s with a step size of 0.01. It can be clearly seen that the controller is able to effectively stabilize the hyperchaotic Lorenz–Stenflo system under consideration. The time variation of control input $u_1$ is shown in Fig. 4.

In the next part of the simulation, synchronization behaviour of two Lorenz–Stenflo systems in master–slave configuration is presented. In this case, simulations are again run for 10 s with a step size of 0.01. The initial conditions for the master system are taken as $\boldsymbol{x}(0) = \begin{bmatrix} 2 & 4 & 6 & 8 \end{bmatrix}^T$ and for the slave system as $\boldsymbol{y}(0) = \begin{bmatrix} 9 & 7 & 5 & 3 \end{bmatrix}^T$, respectively. The synchronization behaviour of corresponding states of the master and the slave systems is depicted in Fig. 5a–d. Convergence of the synchronization errors is shown in Fig. 6. In this case also the feedback gain is taken as $\beta_1 = 2$. The convergence of the synchronization errors to zero indicates that the master and the slave systems are globally asymptotically synchronized for all initial conditions. The variation of control input $u_1$ with time depicting the switching behaviour of the controller is shown in Fig. 7.

Further, synchronization operation is achieved taking into consideration uncertainties in the slave system parameters. In this case, the simulations are run for 8 s. Initial conditions for the adaptation laws of uncertain system parameters are taken as $\tilde{b}(0) = \tilde{c}(0) = 5$. The other positive constants governing the adaptation process of uncertain system parameters are taken as $\eta_1 = \eta_2 = 15$. Figure 8a–d represents the time response of corresponding states of the master and the slave systems with uncertain system parameters. For the same case, convergence of synchronization errors to zero is depicted in Fig. 9, which implies that the objective of synchronization has been achieved. Variation of control input $u_1$ with time is presented in Fig. 10. Convergence behaviour of estimates of uncertain parameters to their true values is presented in Fig. 11. It can be clearly observed from the simulation results that the proposed controller is able to establish synchronization between the master and the slave systems in uncertain environment, which justifies the effectiveness of the proposed strategy.

## 7 Conclusion

The problem of stabilization and synchronization of a class of chaotic and hyperchaotic systems in master–slave configuration, using proportional-integral (PI) surface based SMC scheme is addressed in the manuscript. A sliding mode controller is presented to ensure the occurrence of sliding motion for both stabilization and synchronization cases. The presented analytical procedure helps in deciding the minimum number of control inputs required to stabilize and synchronize the system of the proposed class. It has been shown that with the proper choice of number of control inputs and their parameters, the master and the slave systems get completely synchronized. By using SMC based control inputs, convergence of errors to zero with time has been ensured. Taking into consideration the practical aspects of uncertain environment in which the systems may have to operate, effects of limited parametric uncertainties, is also taken into account. Further, convergence of uncertain parameters to their true values is also achieved. Numerical simulations in support of theoretical results are given in order to show the effectiveness of the proposed strategy.

## References


1. Lorenz EN (1963) Deterministic periodic flow. J Atmos Sci 20(2):130–141
2. Ueta T, Chen G (2000) Bifurcation analysis of Chen's equation. Int J Bifurc Chaos Appl Sci Eng 10(8):1917–1931
3. Lu J, Chen G (2002) A new chaotic attractor coined. Int J Bifurc Chaos Appl Sci Eng 12(3):659–661
4. Morgul O, Solak E (1996) Observer based synchronization of chaotic systems. Phys Rev E 54(5):4803–4811
5. Xiong X, Wang J (2009) Conjugate Lorenz-type chaotic attractors. Chaos Solitons Fractals 40(2):923–929
6. Ott E, Grebogi C, York JA (1990) Controlling chaos. Phys Rev Lett 64(11):1196–1199
7. Liu X, Shen XS, Zhang H (2012) Multi-scroll chaotic and hyperchaotic attractors generated from Chen system. Int J Bifurc Chaos 22(2):1250033 (1-15)
8. Koliopanos CL, Kyprianidis IM, Stouboulos IN, Anagnostopoulos AN, Magafas L (2003) Chaotic behaviour of a fourth-order autonomous electric circuit. Chaos Solitons Fractals 16(2):173–182
9. Cang S, Qi G, Chen Z (2010) A four-wing hyper-chaotic attractor and transient chaos generated from a new 4-D quadratic autonomous system. Nonlinear Dyn 59(3):515–527
10. Yang CC (2011) Adaptive synchronization of Lu hyperchaotic system with uncertain parameters based on single-input controller. Nonlinear Dyn 63(3):447–454
11. Han C, Yu S, Wang G (2015) A sinusoidally driven Lorens system and circuit implementation. Math Probl Eng 2015, Article ID 706902, 11 pages
12. Sun K, Liu X, Zhu C, Sprott JC (2012) Hyperchaos and hyperchaos control of the sinusoidally forced simplified Lorenz system. Nonlinear Dyn 69(3):1383–1391
13. Wang X, Wang M (2008) A hyperchaos generated from Lorenz system. Phys A Stat Mech Appl 387(14):3751–3758
14. Mareca MP, Bordel B (2017) Improving the complexity of Lorenz dynamics. Complexity 2017, Article ID 3204073, 16 pages
15. Chang SC, Lue YF (2017) A study of the nonlinear response and chaos suppression in a magnetically levitated system. Aust J Mech Eng. https://doi.org/10.1080/144844846.2017.1410961
16. Shang H, Wen Y (2013) Suppression of chaos in a MEMS resonator by delayed position feedback. Theor Appl Mech Lett 3:063008
17. Po WH, Jie L, Kun Z (2007) Stability anf Hopf bifurcation of the maglev system with delayed speed feedback control. Acta Automatica Sinica 33:829–834
18. Zhang L, Huang L, Zhang Z (2010) Hopf bifurcation of the maglev time-delay feedback system via pseudo-oscillator analysis. Math Comput Model 52(5–6):667–673
19. Eli KB (1985) On the stability of coupled chemical oscillators. Phys D 14:242–252
20. Dolink M, Epstein IR (1996) Coupled chaotic chemical oscillators. Phys Rev E 54:3361–3368
21. Atanasova T, Zimliki K, Bertram CL, Sherman R (2006) Diffusion of calcium and metabolites in pancreatic islets: killing oscillations with a pitchfork. Biophys J 90:3434–3446
22. Koseska A, Volkov E, Kurths J (2010) Parameter mismatches and oscillation death in coupled oscillators. Chaos 20:023132
23. Ozden I, Venkataramani S, Long MA, Connors BW, Nurmikko AV (2004) Strong coupling of nonlinear electronic and biological oscllators: reaching the "amplitude death" regime. Phys Rev Lett 93:158102
24. Kamal NK, Sinha S (2015) Emergent patterns in interacting neuronal sub-population. Commun Nonlinear Sci Numer Simul 22:314–320
25. Ma J, Song X, Jin W, Wang C (2015) Autapse-induced synchronization in a coupled neuronal network. Chaos Solitons Fractals 80:31–38
26. Wei M, Lun J (2007) Amplitude death in coupled chaotic solid-state lasers with cavity-configuration-dependent instabilities. Appl Phys Lett 91:061121
27. Kim MY, Roy R, Jl Aron, Carr TW, Schwartz IB (2005) Scaling behaviour of laser population dynamics with time-delayed coupling: theory and experiment. Phys Rev Lett 94:088101
28. Kumar P, Parshad A, Ghosh R (2008) Stable phase-locking of an external-cavity diode laser subjected to external optical injection. J Phys B At Mol Opt Phys 1:35402
29. Sharma BB, Kar IN (2009) Parametric convergence and control of chaotic system using feedback linearization. Chaos Solitons Fractals 40(3):1475–1483
30. Chuandong L, Xiaofeng L, Tingwen H (2007) Exponential stabilization of chaotic systems with delay by periodically intermittent control. Chaos 17:013103 (1)–013103 (7)
31. Niu H, Ma S, Fan T, Chen C, He P (2014) Linear state feedback stabilization of unified hyperchaotic systems. World J Model Simul 10(1):34–48
32. Liao TL, Tsai SH (2000) Adaptive synchronization of chaotic systems and its application to secure communication. Chaos Solitons Fractals 11(9):1387–1396
33. Pecora LM, Carroll TL (1990) Synchronization in chaotic system. Phys Rev Lett 64(8):821–824
34. Pecora LM, Carroll TL (1998) Master stability functions for synchronized coupled systems. Phys Rev Lett 80:2109–2112
35. Arenas A, Guilera AD, Kurths J, Moreno Y, Zhou C (2008) Synchronization in complex networks. Phys Rep 469(3):93–153
36. Hong H, Choi MY, Kim BJ (2002) Synchronization on small-world networks. Phys Rev E 65:026139
37. Vincent UE, Njah AN, Solarin ART (2006) Phase synchronization in bi-directionally coupled chaotic ratches. Phys A 360(2):186–196
38. Yanchuk S, Maistrenko Y, Mosekilde E (2001) Partial synchronization and clustring in a system of diffusively coupled chaotic oscillators. Math Comput Simul 54(6):491–508

39. Ge ZM, Chang CM (2009) Generalized synchronization of chaotic systems by pure error dynamics and elaborate Lyapunov function. Nonlinear Anal Theory Methods Appl 71(11):5301–5312
40. Li Z, Xu D (2004) A secure communication scheme using projective chaos synchronization. Chaos Solitons Fractals 22(2):477–481
41. Naderi B, Kheiri H (2016) Exponential synchronization of chaotic system and application to secure communication. Optik Int J Light Electron Opt 127(5):2047–2412
42. Wang Y, Feng X, Lyu X, Li Z, Liu B (2016) Optimal targeting of nonlinear chaotic systems using a novel evolutionary computing strategy. Knowl Based Syst 107:261–270
43. Moran ME, Cosenza MG, Gullen P, Coutin P (2007) Synchronization and clustering in electroencephalographic signals. Chaos Solitons Fractals 31:820–825
44. Smaoui N, Karouma A, Zribi M (2013) Adaptive synchronization of hyperchaotic Chen system with application to secure communication. Int J Innov Comput Inform Control 9(3):1127–1144
45. Singh PP, Singh JP, Roy BK (2014) Synchronization and anti-synchronization of Lu and Bhalekar—Gejji chaotic systems using nonlinear active control. Chaos Solitons Fractals 69:31–39
46. Sharma BB, Kar IN (2010) Contraction theory-based recursive design of stabilising controller for a class of nonlinear systems. IET Control Theory Appl 4(6):1005–1018
47. Handa H, Sharma BB (2016) Synchronization of a set of coupled chaotic FitzHugh–Nagumo and Hindmarsh–Rose neurons with external stimulation. Nonlinear Dyn 85(3):1517–1532
48. Bowong S (2007) Adaptive synchronization of chaotic systems with unknown bounded uncertainties via backstepping approach. Nonlinear Dyn 49(1):59–70
49. Vargas JAR, Grzeidak E, Gulrate KHM, Alfaro SC (2016) An adaptive scheme for chaotic synchronization in the presence of uncertain parameters and disturbances. Neucomputing 174(part B):1038–1048
50. Handa H, Sharma BB (2016) Novel adaptive synchronization scheme for a class of chaotic systems with and without parametric uncertainty. Chaos Solitons Fractals 86:50–63
51. Handa H, Sharma BB (2011) Stabilization and synchronization of MLS chaotic system using PI based sliding mode control, Bali, Indonesia. TENCON-2011, pp 1095–1099
52. Zhang H, Ma XK (2004) Synchronization of chaotic systems with parametric uncertainty using active sliding mode control. Chaos Solitons Fractals 21(5):1249–1257
53. Yan JJ, Yang YS, Chiang TY, Chen CY (2007) Robust synchronization of unified chaotic system via sliding mode control. Chaos Solitons Fractals 34(3):947–954
54. Ablay G (2009) Sliding mode control of uncertain unified chaotic systems. Nonlinear Anal Hybrid Syst 3(4):531–535
55. Roopaei M, Sahraei BR, Lin TC (2010) Adaptive sliding mode control in a novel class of chaotic systems. Commun Nonlinear Sci Numer Simulat 15(12):4158–4170
56. Ghamati M, Balochian S (2015) Design of adaptive sliding mode control for synchronization Genesio–Tesi chaotic system. Chaos Solitons Fractals 75:111–117
57. Lorenz EN (1963) Deterministic nonperiodic flow. J Atmos Sci 20:130–141
58. Li Y, Liu X, Chen G, Liao X (2011) A new hyperchaotic Lorenz-type system: generation, analysis, and implementation. Int J Circ Theor Appl 39:865–879
59. Stenflo L (1996) Generalized Lorenz equations for acoustic gravity waves in the atmosphere. Physica Scripta 53:83–84
60. Wang P, Li D, Hu Q (2010) Bounds of hyper-chaotic Lorenz–Stenflo system. Commun Nonlinear Sci Numer Simul 15(9):2514–2520
61. Utkin VI (1978) Sliding mode and their application in variable structure system. Mir Editors, Moscow
62. Uyaroglu Y, Emiroglu S (2013) Passivity-based chaos control and synchronization of four dimensional Lorenz–Stenflo system via one input. J Vib Control 21(8):1–8
63. Kocamaz UE, Uyaroglu Y (2014) Synchronization of Vilnius chaotic oscillators with active and passive control. J Circuits Syst Comput 23(7):1450103 (1–17)
64. Ates M, Laribi S (2018) New results on the global asymptotic stability of certain nonlinear RLC circuits. Turk J Electr Comput Sci 26:434–441